

QATAR UNIVERSITY

Graduate Studies

College of Arts & Science

**The Role of Key Impurity Elements on the Performance of Aluminium Electrolysis -  
Current Efficiency and Metal Quality**

A Thesis in

Material Science & Technology

By

Jassim Ali Al-Mejali

© 2015 Jassim

Submitted in Partial Fulfillment

of the Requirements

for the Degree of

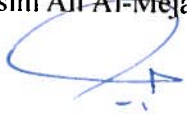
Master of Art & Science

May 2015

## **Declaration**

To the best of my knowledge, this thesis contains no material previously published or written by another person or institution, except where due reference is made in the text of the thesis. This thesis contains no material which has been accepted for the award of any other degree in any university or other institution.

Name: Jassim Ali Al-Mejali

Signature: 

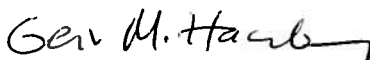
Date: 07 May 2015

## Committee

The thesis of Jassim Ali Al-Mejali was reviewed and approved by the following:

We, the committee members listed below, accept and approve the Thesis of the student named above. To the best of this committee's knowledge, the Thesis confirms the requirements of Qatar University, and we endorse this Thesis for examination.

Main Supervisor: Professor Geir Martin Haarberg

Signature: 

Date: 22 June 2015

Committee Member: Dr. Nasr Bensalah

Signature: 

Date: 24 June 2015

Committee Member: Dr. Aboubakr Ali

Signature: 

Date: June 24, 2015

Committee Member: Professor Hans Roven

Signature:

Date:

Committee Member: Mr. Ben Benkahla

Signature: 

Date: June, 22<sup>nd</sup> 2015

## Abstract

Impurities such as phosphorus and silicon mainly enter the aluminium electrolysis process with alumina. These impurities dissolve in the electrolyte and affect the performance of the electrolysis, the emissions from the cells and the quality of the metal produced. In the present work, the behavior of phosphorus and silicon species in the industrial Hall-Héroult cells was investigated. The study was based on the deleterious effect of phosphorus and silicon on the aluminium production process. It is established in the literature that for every 100 ppm of phosphorus in the bath the current efficiency is decreased by 1%.

The chemical and electrochemical behavior of phosphorus and silicon compounds in the Hall-Héroult process was studied. Measurements were as well carried out in QATALUM industrial cells by analysis of bath and metal after addition of phosphorus and silicon compounds to the bath. Additions of  $\text{AlPO}_4$ ,  $\text{Na}_3\text{PO}_4$  and  $\text{SiO}_2$  to the industrial prebaked cells were performed and the variation of the concentration in both the bath and metal was followed over time. Phosphorus showed to have a much longer retention time in the bath than silicon. Variations during start-up of cells and anode effects seemed to influence the phosphorus and silicon level in the cells. From industrial data trends, it can be observed that the amount of phosphorus in the cells decreases with increasing the operating temperature.

It was found that merely small amounts of phosphorus are reduced at the cathode. Unlike phosphorus, large amounts of silicon were primarily reduced at the cathode and ended up in the metal. Mass balance for phosphorus for prebake cells was presented. It was found that a massive amount of the phosphorus entering the cells was transported with the off-gases to the dry scrubbers. Since the secondary alumina is used as feeding for the prebake cells, the phosphorus is recycled back and will end up in the produced metal.

# Contents

List of Tables .....	7
List of Figures .....	8
List of Symbols and abbreviations .....	10
Acknowledgements.....	12
Motivation.....	14
1. Introduction .....	15
1.1 Aluminium Characteristics and Hall-Héroult Production Process .....	15
1.2 Impurities in the aluminium electrolysis process.....	22
1.3 Phosphorus as an impurity .....	28
1.4 Silicon as an impurity .....	29
1.5 Scope of the work .....	30
2. Literature review .....	31
2.1 General chemistry of phosphorus .....	31
2.1.1 Natural occurrence and production of phosphorus.....	31
2.1.2 Compounds of phosphorus in the molten state .....	32
2.2 Phosphorus in industrial aluminium cell.....	34
2.2.1 Laboratory studies .....	36
2.2.2 Industrial studies .....	40
2.3 General chemistry of silicon .....	45
2.3.1 Natural occurrence and production of silicon.....	45
2.3.2 Silicon alloys .....	46
2.4 Silicon in industrial aluminium cell.....	47
3. Theory .....	48
4. Experiment .....	51
5. Results and Discussion.....	55

5.1 Distribution of phosphorus and silicon after addition..... 55

5.2 Phosphorus and process variables..... 62

5.3 Silicon and process variables ..... 65

5.4 Phosphorus and current efficiency..... 67

5.5 Metal Inventory by copper dilution ..... 69

5.6 Current efficiency (%CE) loss calculation..... 70

5.7 Silicon mass transfer coefficient ..... 72

5.8 Phosphorus Mass balance ..... 74

6. Conclusion..... 76

Bibliography ..... 78

Appendix A..... 83

Appendix B..... 90

## List of Tables

<b>Table 1.1:</b> Impurity concentrations in different raw material.....	83
<b>Table 1.2:</b> Impurity concentrations in different raw materials.....	84
<b>Table 1.3:</b> Impurities mass balance and distribution per unit of aluminium metal.....	25
<b>Table 1.4:</b> Impurities concentration and the increase in metal contamination caused by dry scrubber.....	27
<b>Table 2.1:</b> Contents of phosphorus expressed as $P_2O_5$ in different raw materials in ppm.....	34
<b>Table 2.2:</b> Contents of phosphorus expressed as $P_2O_5$ in different raw materials per tonne of aluminium produced in ppm.....	35
<b>Table 2.3:</b> Laboratory data for the distribution coefficients between bath and metal for several impurities, impurity level A equals 0.0025wt.% P, 0.02 wt.% Si and 0.01 wt.% Fe in the bath, impurity level 2A equals twice the impurity concentrations of A and so for impurity fourth and eighth.....	85
<b>Table 2.4:</b> Size and phosphorus concentration analysis of secondary alumina.....	39
<b>Table 2.5:</b> Input.....	86
<b>Table 2.6:</b> Recycling material and bath.....	87
<b>Table 2.7:</b> Output.....	88
<b>Table 2.8:</b> Phosphorus mass balance at Soderberg cells fed by primary $Al_2O_3$ .....	89
<b>Table 2.9:</b> Primary alumina shipments from different suppliers and their phosphorus contents.....	43
<b>Table 5.1:</b> Input.....	74
<b>Table 5.2:</b> Output.....	74

## List of Figures

<b>Figure 1.1:</b> Hall-Héroult cell with prebaked carbon anodes.....	17
<b>Figure 1.2:</b> Hall-Héroult cell with Soderberg carbon anodes.....	18
<b>Figure 1.3:</b> The amount of the main raw materials needed for production of 1 tonne of aluminium.....	21
<b>Figure 1.4:</b> The amount of silicon on the silicon carbide sideling.....	29
<b>Figure 3.1:</b> Mass transport of species $M^+$ from the electrolyte into the produced aluminium.....	48
<b>Figure 4.1:</b> A certain amount of $Na_3PO_4$ , $AlPO_4$ and $SiO_2$ were added in the industrial cells.....	51
<b>Figure 4.2:</b> Bath and metal samples were taken and placed in proper place in able to be analyzed.....	52
<b>Figure 4.3:</b> Bath samples were analyzed by X-ray Fluorescence (XRF).....	52
<b>Figure 4.4:</b> Metal samples were analyzed by automated optical emission spectroscopy (OES).....	52
<b>Figure 4.5:</b> Metal inventory by copper dilution.....	53
<b>Figure 4.6:</b> QATALUM side-by-side prebake cells with 30 anodes.....	54
<b>Figure 5.1:</b> Distribution of phosphorus in the bath as a function of time after adding $AlPO_4$ .....	56
<b>Figure 5.2:</b> Distribution of phosphorus in the metal as a function of time after adding $AlPO_4$ .....	56
<b>Figure 5.3:</b> Distribution of phosphorus in the bath as a function of time after adding $Na_3PO_4$ .....	57
<b>Figure 5.4:</b> Distribution of phosphorus in the metal as a function of time after adding $Na_3PO_4$ .....	57
<b>Figure 5.5:</b> Distribution of silicon in the bath as a function of time after adding $SiO_2$ .....	58
<b>Figure 5.6:</b> Distribution of silicon in the metal as a function of time after adding $SiO_2$ .....	58
<b>Figure 5.7:</b> Distribution of phosphorus and silicon in the bath after the addition.....	59
<b>Figure 5.8:</b> Distribution of phosphorus and silicon in the bath after the addition.....	59
<b>Figure 5.9:</b> Distribution of silicon in the metal and bath after the addition.....	60



**Figure 5.10:** Average values for the phosphorus content in aluminium and bath temperature over time for prebaked pot-line at QATALUM over a period of 1 year.....62

**Figure 5.11:** Correlation between phosphorus concentration in the metal and bath temperature during anode effect.....63

**Figure 5.12:** Correlation between phosphorus concentration in the metal and bath temperature of new cells.....64

**Figure 5.13:** Average values of the silicon concentration in aluminium and bath temperature over time for prebaked pot-line at QATALUM over a period of 8 months.....65

**Figure 5.14:** Correlation between silicon concentration in the metal and bath temperature of new cells.....66

**Figure 5.15:** Correlation between sodium concentration in the produced aluminium and the current efficiency (%CE).....67

**Figure 5.16:** Correlation between phosphorus and sodium content in the produced metal for the experimental cells.....68

**Figure 5.17:** The average values of the metal inventory by copper dilution for the experimental cells at QATALUM over a period of one year.....69

**Figure 5.18:** Correlation between Na concentration in the produced aluminium and the current efficiency (%CE).....70

**Figure 5.19:** Log concentration of silicon impurity in the bath as a function of time after additions of SiO<sub>2</sub>.....72

**Figure 5.20:** Mass balance for phosphorus. The phosphorus content in the various mass flows for a typical prebake QATALUM cell.....75

# List of Symbols and abbreviations

## Symbols

Symbol	Meaning	Unit
$E^{\text{rev}}$	Reversible potential	V
$E^{\circ}$	Standard potential	V
K	Equilibrium distribution coefficient	
$i_l$	Limiting current density	$\text{A.cm}^{-2}$
$c^{\circ}$	Bulk concentration	$\text{Mol.cm}^{-3}$
k	Mass transfer coefficient from bath into metal	$\text{m.s}^{-1}$
$C_{\text{bath}}$	Concentration in bath	ppm
$C_{\text{boundary}}$	Concentration at boundary interface	ppm
$c_o$	Background concentration	ppm
V	Volume of electrolyte	$\text{m}^3$
J	Flux	$\text{mol.cm}^{-2}.\text{s}^{-1}$
I	Current	A
A	Area of cathode	$\text{m}^2$
$C_{\text{cu}}$	Purity of copper added	ppm
$M_{\text{cu}}$	Quantity of copper added	g
$C_1$	Concentration of copper before addition	ppm
$C_2$	Concentration of copper after addition	ppm

## Abbreviations

Abbreviation	Meaning
%CE	Current efficiency
CA	Anode change
AE	Anode effect
ACD	Anode cathode distance
XRF	X-ray fluorescence
OES	Automated optical emission spectroscopy
SHE	Standard hydrogen electrode (1 atm, 25 °C)

## **Acknowledgements**

The present work was carried out between 2014 and 2015 at the College of Arts and Sciences in Qatar University under the supervision of Professor Geir Martin Haarberg and Dr. Nasr Bensalah.

First of all, I would like to thank my main supervisor Professor Geir Martin Haarberg for his guidance, support and encouragements in scientific field. Again, sincere gratitude for the information provided, helpful discussions, kindness and patience during the research period.

My sincere appreciation goes to Dr. Nasr Bensalah from Department of Chemistry and Earth Sciences who co-supervised this work and was at any time, willing to spare his time to encourage and discuss with me on the subject matter. I am appreciative for his advice and active guidance.

Similarly my appreciation goes to supportive staff at the Center of Advanced Materials (CAM) and Material Science and Technology Program at Qatar University particularly Dr. Aboubakr Ali and Professor Hans Roven for their assistance every time when needed.

A special thank goes to Mr. Ben Benkahla from Department of Reduction at Qatar Aluminium Company (QATALUM) in Qatar for giving me the possibility of carry out experiment on impurities addition in QATALUM industrial cells. Also, I would like to express my gratitude for taking his time to read through my thesis and whose comments and advices were highly helpful.

Since the study performed industrial measurements at QATALUM plant I would like to thank Mr. Hans Petter Lange, Mr. Abhay Dhuwe, Mr. Ali Zaid, Mr. Slawomir Grenda and Mr. Pedro Cumbane for their interest and help. Also, Qatar Aluminium Company (QATALUM) is appreciatively acknowledged for their financial support.

I would like to thank Mr. Madhu Ramakrishnan and Mr. Vikas Goswami from QATALUM and Mr. Essam from Qatar University who assisted me with the practical matters in laboratory.

I am deeply grateful to all people and colleagues from Material Science and Technology Master Program who gave me warm welcome to their group and has since been my friends. Specifically, I am very thankful to Ms. Sharon Sonia who took care of administrative concerns anytime I asked for her assistance.

Finally, I would like to thank my wife, parents and family for all their love, support, understanding and optimism and encouragement during these years. I really appreciate it.

Jassim Al-Mejali

Doha, May 2015

## Motivation

It is important to highlight that this research represents good initiative collaboration between Qatar University and QATALUM. This will open new opportunities for students, faculties and researchers to profound scientific cooperation to solve real and actual problems, and it will strengthen the partnership recently established between Qatar University and QATALUM.

In all smelters, current efficiency (%CE) is one of the most important parameter as it shows the technical performance of the cells but also has an important impact on the financial results. Impurities are one of the critical root causes that impact significantly the current efficiency. Thus, it is important to have a structured approach from the QATALUM's management toward this technical aspect. As in most of the smelters, QATALUM is facing a specific issue regarding its Basement Anode Cover Mix Material. As this material has a significant financial value, there is a project for recycling it into the process loop.

However, this material can have negative impacts on the cell performance in terms of current efficiency and metal quality due to the presence of impurities such as phosphorus and silicon. This project will contribute to the good understanding of the behavior of such impurities by studying their effects on the cell performance.

Future raw materials, mainly alumina and anode carbon, may contain more impurities. Modern cells are designed to reduce the emissions. Therefore, it may become challenging to reduce the impurity level in the produced metal. It is important to understand the behavior of impurities during industrial electrolysis, and the impact of impurities on important process parameters.

# Chapter 1

## 1. Introduction

The interest for phosphorus and silicon in aluminium production technology has considerably increased as the cell design has modified to closed systems and dry scrubbers especially when recycling of alumina was introduced. The current efficiency for aluminium in modern cells is typically ranging between 90 and 96%. Further, increase in the current efficiency depends on improving a number of factors. One of these factors is the behavior of impurities in the cells especially for phosphorus and silicon. For every 100 ppm phosphorus in the electrolyte, the current efficiency is reduced by about 1% [1]. Moreover, there is a limit on the phosphorus and silicon contents in aluminium mainly for cast alloys. To evade further tribulations caused by phosphorus and silicon content, it is essential to improve the understanding of the behavior of phosphorus and silicon in Hall-Héroult process cells.

### 1.1 Aluminium Characteristics and Hall-Héroult Production Process

Aluminium is the world most abundant metal and it is the third major ordinary element which comprise to 8% of the earth's crust. The usefulness of aluminium causes it the main commonly utilized metal following steel. The international demand for aluminium metal has risen to more or less 55 million tonnes per year [1]. The total world production of primary aluminium was more than 56 million tonnes in 2014 [1]. Approximately 18 million tonnes are annually recycled as scrap [1].

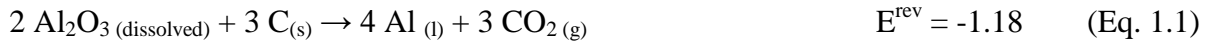
Aluminium is soft, light in weight, and apparently dull silver. It is remarkable for its superior strength corrosion resistance due to the protecting oxide layer. Aluminium is about one-third as dense as steel and it is the second major malleable metal after gold and the sixth major ductile. It has also excellent electrical and thermal properties.

By utilizing different combinations of its useful characteristics such as lightness, strength, corrosion resistance and recyclability, aluminium has been used in different applications in a number of industries. In addition to these, Aluminium is used in the production of transport vehicles, building construction and electrical engineering applications. To conceptualize its use and functions, it has found its utilizations in packaging applications. Development in industrial application has indicated that there are possibilities of forming alloys with various elements such as zinc, manganese and copper to provide the higher strengths which makes it even very important to the world economy.

Even though aluminium compounds have been utilized for hundreds of years, aluminium metal was first produced about 150 years ago. This is because in nature, aluminium is found only in an oxidized form due to its higher affinity for oxygen and exists in very stable combinations with other materials. Today, the only industrially used way of aluminium production is the Hall-Héroult process. It was invented in 1886 independently by Paul Louis Héroult (France) and Charles Martin Hall (USA). The process is based on electrochemical decomposition of aluminium oxide which is called alumina ( $\text{Al}_2\text{O}_3$ ). Since aluminium cannot be deposited cathodically in water solution, molten cryolite ( $\text{Na}_3\text{AlF}_6$ ) is used as a solvent. The Hall-Héroult process is far from being an ideal industrial process due to low energy efficiency and environmental impact. For this reason, a number of attempts to evolve new ways of aluminium production have been made. Nevertheless, until today aluminium is produced solely by the Hall-Héroult process. Even though there have been a number of significant improvements in its production, the fundamental basis remains the same.

In the Hall-Héroult process, aluminium is produced electrolytically according to the overall Eq. 1.1. Alumina ( $\text{Al}_2\text{O}_3$ ) is used as the source of aluminium. Carbon is coming from consumable anodes made from a petroleum coke. An alternative is the usage of oxygen evolving and environmentally friendly inert anodes as in Eq. 1.2. Inert anodes are still under research. In industrial production, only carbon anodes are used today.





Today, two types of anode design are in use: the prebaked anodes which have been commonly used during the last decades due to their operational advantages and the self-baking Soderberg anodes. The modern Hall-Héroult electrolysis cell with prebaked carbon anodes is shown in Figure 1.1. Most of the cells have typically 20 to 40 prebaked anodes per cell positioned horizontally in the bath. However, in Soderberg anode, only a single continuous self-baking anode is used as shown in Figure 1.2. The prebaked anode is made from a mixture of petroleum coke aggregate and coal tar pitch as binder and baked in separate anode baking furnaces at about 1200°C. Conversely, the Soderberg anode is produced from petroleum coke and higher content of coal tar pitch and is continuously baked in the electrolysis cell.

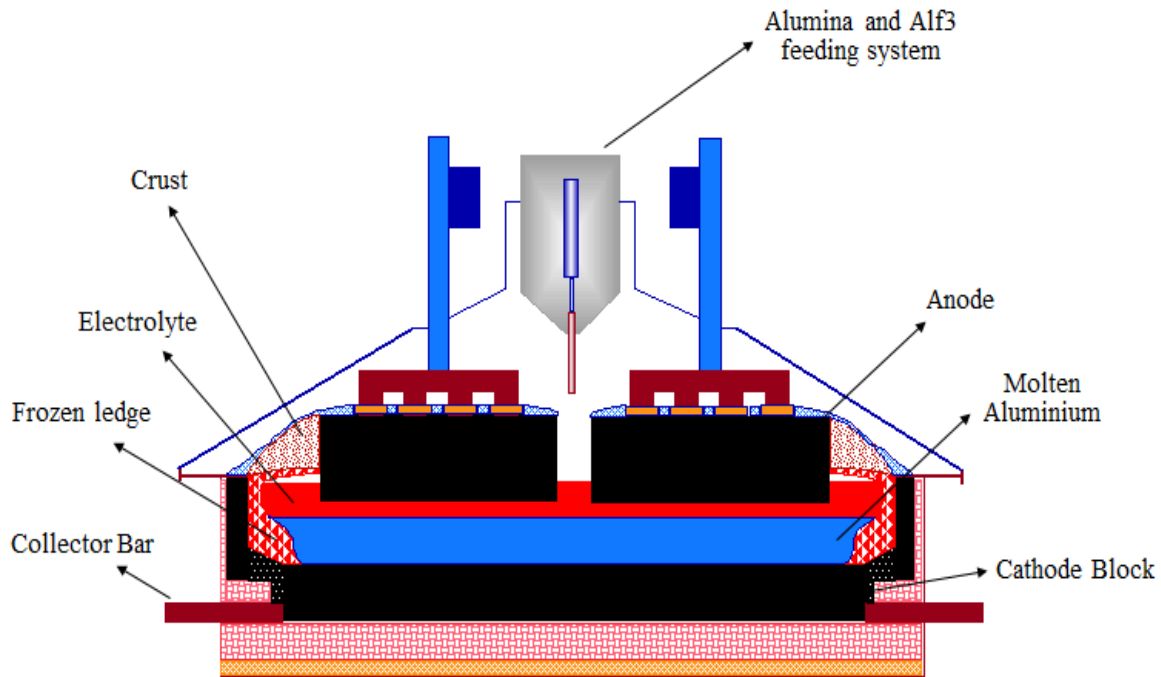


**Figure 1.1:** Hall-Héroult cell with prebaked carbon anodes [2]

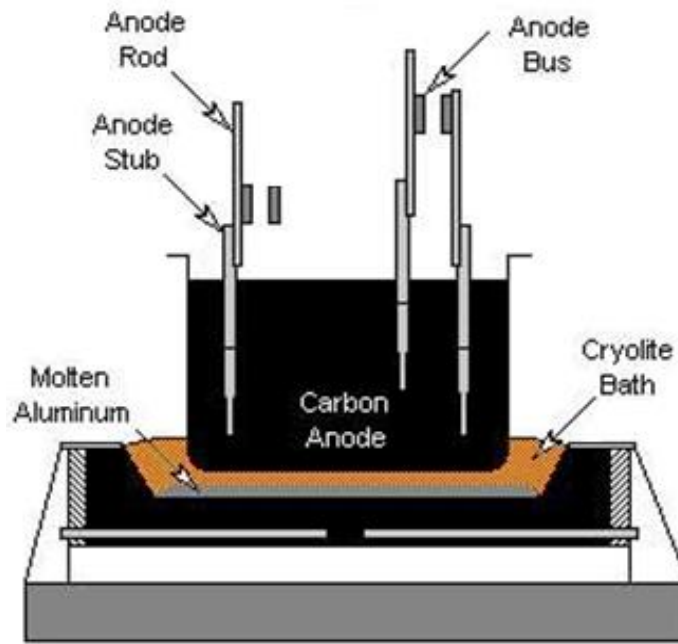


**Figure 1.2:** Hall-Héroult cell with Soderberg carbon anodes [2]

Modern aluminium plants operate with 100-300 cells connected in series mostly side by side to reduce the magnetic effects. The aluminium production in Hall-Héroult electrolysis cell is a continuous process. Alumina ( $\text{Al}_2\text{O}_3$ ) is fed to the cell continuously and the produced metal is usually tapped once per day. Another regularly added material is aluminium fluoride ( $\text{AlF}_3$ ). Prebaked anodes need to be changed regularly because they are consumed to a certain extent. After 20-30 days, prebaked anodes have to be replaced by new ones. Soderberg anode is produced continuously over the whole cell life time.

The molten aluminium metal pad serves as cathode. The prebaked reduction cell consists of outer steel shell, insulation bricks, carbon cathode blocks, side lining made from silicon carbide and a superstructure holding the anodes. The side lining is protected against corrosion by a layer of frozen bath (cryolite) called side ledge. The top of the cell around the anodes is covered by the crust from frozen bath and alumina. This crust serves as the first step of anode gas filtration. Crust materials are removed from the cell when anodes are changed and replaced by a new cover mixed.

The main purpose of the bath is to dissolve alumina. Also, it has low density, low resistivity and low metal solubility. The principle constituent of the bath in Hall-Héroult electrolysis cell is molten cryolite. This cryolite is used because of its good solvent properties for alumina. It dissociates in molten phase into  $\text{Na}^+$  and  $\text{AlF}_6^{3-}$  ions. A fraction of the latter complexes dissociate further into  $\text{F}^-$ ,  $\text{AlF}_4^-$  or  $\text{AlF}_5^{2-}$ . Aluminium ions bound in such fluoride complexes are transported by diffusion to the cathode and discharged at the electrolyte-metal interface according to equation 1.3 and equation 1.4.



Sodium cations migrate toward the cathode and NaF diffuses back to the electrolyte. Even though the sodium ions carry most of the charge through the electrolyte, for electrochemical reasons aluminium deposition is favored over sodium. Besides cryolite, the electrolyte is usually modified by additives which improve the properties such as increased electrical conductivity, lower metal solubility, and lower melting temperature of the bath. The commonly used additives are calcium fluoride ( $\text{CaF}_2$ ) and aluminium fluoride ( $\text{AlF}_3$ ). Typical concentration of  $\text{CaF}_2$  is 4-6 wt.%. This builds up in bath spontaneously because calcium is a common impurity in alumina. Excess  $\text{AlF}_3$  is used in amount ranging from 3-15 wt.% depending on cell design. For instance, Soderberg cells operate at lower  $\text{AlF}_3$  content than prebaked cell. The surplus of  $\text{AlF}_3$  in the melt is normally expressed as a cryolite ratio or as a bath ratio. Unfortunately, excess  $\text{AlF}_3$  lowers the solubility of  $\text{Al}_2\text{O}_3$ . Typical alumina concentration is 2-4 wt.%. In some cases, 2-4 wt.%  $\text{LiF}$  and  $\text{MgF}_2$  are used as additives as well. The operating temperature depends on the bath composition and cell design and usually it ranges between 950-960°C.

Aluminium oxide or alumina used as principle raw materials is produced from bauxite by the Bayer process. In the Bayer plant, bauxite is digested by hot solution of NaOH under pressure. Aluminium from bauxite

dissolves in liquor as sodium aluminates ( $\text{NaAlO}_2$ ) while the insoluble rest of bauxite mainly iron oxides are filtered out as red mud. The liquor is then cooled and  $\text{Al}(\text{OH})_3$  precipitated. Finally, the precipitate is filtered and calcined in rotary kiln to  $\text{Al}_2\text{O}_3$ . Bauxite contains largely  $\text{Al}_2\text{O}_3$  ranges 40-60% found in the hydrous phases. Alumina is fed to the Hall-Héroult electrolysis cell through point feeders in regular intervals to keep its concentration within the range 2-4 wt.%. If the amount of  $\text{Al}_2\text{O}_3$  is insufficient, anode effect may occur. This leads to increase in the cell voltage at which the fluoride components of the bath decompose which results in an increase of the emissions and reduced current efficiency.

In most of aluminium plants, anode gases are treated in so called dry scrubbers. In dry scrubbers, anode gases are passing through primary alumina. HF and other F containing gaseous species from anode gases are adsorbed on  $\text{Al}_2\text{O}_3$ . The HF trapping on alumina lowers the fluoride losses and protects the environment from the emission. Furthermore, solid particles such as carbon dust from anode gases are attached on alumina by electrostatic force. Thus, dry scrubber dramatically influences the impurity distributions and behaviors in the aluminium production process.

The production capacity of modern cells is about 2000 kg Al per day. Typical material consumption for 1 tonne of aluminium produced is about 400-500 kg of carbon, 1900-2000 kg of alumina and 20-30 kg of aluminium fluoride as shown in Figure 1.3. Nowadays, plants are operating up to 96% current efficiency. The feasibility of obtaining such high current efficiency is limited by raw materials quality, cell design and cell control system. The best results are obtained in modern prebaked cells which operate at low temperature, high acidity and have stable metal pad causing slow transport of dissolved metal from cathode to bath. Even though the current efficiency is very high, the energy efficiency of the electrolysis process carried out in cell design is about 45% maximum. The theoretical energy consumption is 6.34 KWh/kg Al while the real value is about 14 KWh/kg Al [2]. Most of the spent energy is lost as heat due to ohmic resistances in the bath and electrodes as well as due to overvoltage. The typical cell voltage of a prebaked cell is 4.1 to 4.5 V while the voltage needed for the aluminium production is about 1.8 V.

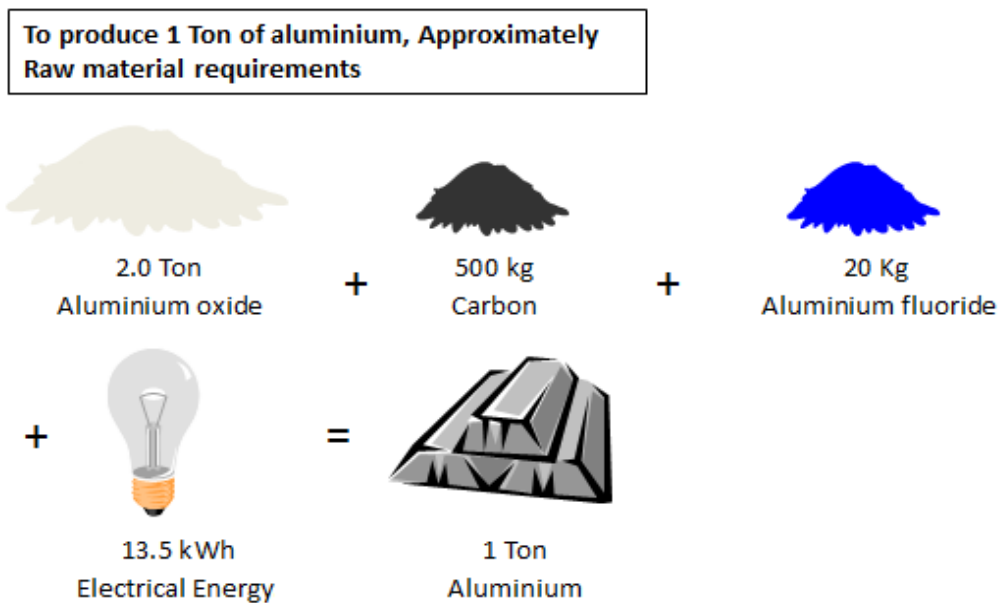
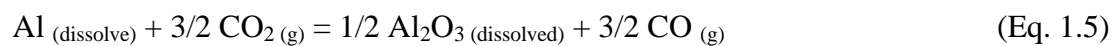


**Figure 1.3:** The amount of the main raw materials needed for production of 1 tonne of aluminium [2]

The main loss in current efficiency is due to the back reaction between dissolved metal and the anode gas as shown in Eq. 1.5. The other reasons for the decrease in current efficiency are the earlier mentioned anode effect, electronic conductivity of the bath due to dissolved Na, electrode short circuiting and impurities. The decrease in the current efficiency caused by the impurities can be 2% in a normal Hall-Héroult electrolysis cell.



## 1.2 Impurities in the aluminium electrolysis process

Primary metal usually has a purity of 99.5 to 99.9 % Al [3]. The rest is species introduced to the electrolysis cells called impurities. The impurities are fed to the electrolyte together with the raw materials such as alumina, carbon anodes, fluorides and the cryolite. Some of these impurities come up from the cell operation or from the production tools. For instance, additional source of iron is from corrosion of tools or anode stubs. Silicon can also come from the refractory lining or silicon carbide sideling. All the impurities to a varying degree have an effect on the electrolysis process.

Impurities more noble than aluminium decompose electrolytically and reduce on the cathode and contaminate the produced aluminium metal or they may be deoxidized at the anode and cause decrease in the current efficiency. Impurities less noble than aluminium will accumulate in the electrolyte where they can react with the components in the bath and thus modify the chemical composition of the melt. Also, they could interact with the carbon in the anodes or lining. Other impurities not so detrimental to the aluminium production process are those which escape from the cell as harmful gases. Nevertheless, they do not accumulate in the electrolyte or in the aluminium metal. As such, they do not decrease the current efficiency or lower the metal quality. However, they have negative impact on the environment. Typical impurity concentrations data from different raw materials are listed in Table 1.1 and Table 1.2 in Appendix A.

The major part of the impurities dissolves in the electrolyte while the minor part leaves the cell as outlet in various ways; in the contaminated aluminium metal, as off gases or adsorbed on carbon dust, alumina or other materials that are skimmed off. However, a significant amount of the impurities is recycled back to the electrolysis process mainly due to the dry scrubber where gaseous and particulate impurities are collected and recycled.

The behavior of particular impurity elements in the process depended on a number of factors. For example, it depends on the decomposition potential of an impurity compound as well as volatility of present species.

Grjotheim et al. [4] classified the impurities according to their nature and behavior in the electrolysis process.

They divided them into several groups as follows:

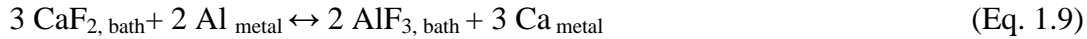
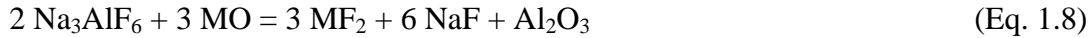
- 1- Water as an impurity
- 2- Metal oxides with higher decomposition potential than alumina ( $\text{Al}_2\text{O}_3$ )
- 3- Metal oxides with lower decomposition potential than alumina ( $\text{Al}_2\text{O}_3$ )
- 4- Non-metallic impurities
- 5- Sulphur containing compounds

Water is adsorbed in raw materials (alumina and fluorides) or enters the electrolyte by atmospheric moisture [4]. Water causes hydrolysis of fluorides in bath which can be expressed by Eq. 1.6. Thus leading to losses in fluoride and environment related problems. However, nowadays most of the smelters are equipped with dry scrubber which recycles fluorides back to the electrolysis cells. As well, water in electrolyte may be decomposed by aluminium metal according to Eq. 1.7. The resulting hydrogen dissolves in the aluminium metal and deteriorates its casting properties [4]. The electrochemical cathodic formation of hydrogen is also possible.



Typical metal oxides with higher decomposition potential than alumina are alkali and alkaline earth oxides. Theoretically, they should not interfere with the cathodic process; however, they are able to react with dissolved oxide in the bath according to Eq. 1.8. This reaction leads to fluoride formation and increasing aluminium fluoride consumption. Nevertheless, if the concentration of this type of metal oxide is sufficiently high to reduce the difference between the deposition potentials of the metal and aluminium, co-deposition of such metal is also possible according to Eq. 1.9 which will decrease the current efficiency of the electrolysis

process. One example is calcium ions which come from alumina. Partly,  $\text{Ca}^{2+}$  leaves the electrolyte cell in the gas phase and is deposited in the produced aluminium but some of them diffuse away through the cathode. After some time, the calcium level reaches a steady state concentration in the electrolyte.



Other common examples of this group of oxides are  $\text{Mg}^{2+}$ ,  $\text{Li}^+$  and  $\text{Na}^+$  oxides. The sodium concentration in alumina is rather high due to the Bayer process where NaOH is used for bauxite extraction. Alkali and alkaline earth metals as impurities in the raw materials do not cause any serious problems in aluminium electrolysis process. Nonetheless, these metals can penetrate into the carbon cathode and cause serious deterioration of the cell lining which contribute to shorter cell life time.

The third group of impurities is represented by the metal oxides with lower decomposition potentials than alumina which concerns most metals except alkali and alkaline earth metals. Most common are oxides of Fe, Si, Ga, V and Ni. They are present in alumina, carbon anode and some originate from tools and production equipment. These metals are nobler than aluminium and tend to be deposited at the cathode electrochemically according to Eq. 1.10. Hence, they are responsible for most of the contamination of the produced metal. The most important aluminium contaminants are Fe and Si.



Jentoftsen [5] studied the transport of Fe, Si, and Ti from electrolyte to aluminium metal in industrial electrolysis cell. These cathode reactions were found to be mass transfer controlled. Fe affects the mechanical properties, re-crystallization, deformation and conductance of the produced metal. For some other impurities



such as Zn, Cu and V, the maximum concentrations in the final product are specified and must be strictly met because of their negative influence on the quality of the final product. All impurities of this group decrease the current efficiency of the electrolysis process due to the consumption of current which otherwise can be used for aluminium production or due to the reduction of aluminium consumed by the reaction as in Eq. 10. Also, these impurities unlike the alkali and alkaline earth oxides do not accumulate in the electrolyte (bath); however, they are transferred to the metal. In fact, a large proportion of them escapes from the electrolysis cell in the form of volatile compounds as listed in Table 1.3 or they are attached to the carbon dust. The role of silicon species in aluminium production technology is discussed in details in Chapters 1.4 and 2.

**Table 1.3:** Impurities mass balance and distribution per unit of aluminium metal [6]

<b>Input (ppm)</b>	<b>Fe</b>	<b>Si</b>	<b>Ga</b>	<b>Ti</b>	<b>Zn</b>	<b>V</b>	<b>P</b>
Alumina	348	123	131	67	60	24	16
Carbon	227	173	2	3	1	33	4
Bath components	31	19		1		2	5
Miscellaneous	223	200					
<b>Feed Sum</b>	<b>829</b>	<b>515</b>	<b>133</b>	<b>71</b>	<b>61</b>	<b>59</b>	<b>25</b>
<b>Output (ppm)</b>							
Metal	451	473	65	25	48	20	3
Gas	378	42	66	41	12	38	18
<b>Total Sum</b>	<b>829</b>	<b>515</b>	<b>131</b>	<b>66</b>	<b>60</b>	<b>58</b>	<b>21</b>

The 4<sup>th</sup> group of impurities according to the classification is non-metallic oxides. Boron and phosphorus oxides are the main representative of the non-metallic oxides group. Boron has favorable effect on the quality of the aluminium final product because it helps in the reduction of the content of heavy metals. Sometimes, it is added to the aluminium to remove Ti and V as deposited borides [7]. However, phosphorus oxides are one

of the most dangerous impurities.  $P_2O_5$  can be reduced both electrochemically and chemically by Al. Even at low concentration, it lowers the corrosion resistance and increases the brittleness of the final product. The most remarkable negative effect of  $P_2O_5$  is the decrease in current efficiency. It was reported that 100 ppm of phosphorous in the electrolyte can lower the current efficiency by about 1% [1]. Another negative effect of phosphorus oxides on the electrolysis process is the improvement of wetting of dispersed carbon particles in the electrolyte which leads to overheating of the electrolyte. The role of phosphorus in aluminium production technology is discussed in details in Chapters 1.3 and 2.

The last and very significant impurity in aluminium electrolysis process is sulphur and sulphur containing species. They are introduced into the process together with the raw materials mainly in anodes and leave the cell as harmful and environmentally polluting gases. Sulfur concentration in petrol coke is about 4 wt.% and is present in coke in various organic compounds such as  $C_4H_4S$  [8]. Sulphur leaves the electrolytic cell as gaseous species such as  $SO_2$ ,  $H_2S$  and  $CS_2$ . These species need to be removed from the outgoing gas stream due to their environmental impacts. Usually,  $SO_2$  is trapped by absorption in wet scrubber. Fellner et al. [9] studied the behavior of sulphur in the electrolyte. They studied the chemical reduction of sulphate anion by carbon and metallic Al. Sulphides and poly-sulphides were found to be products of chemical reaction. Concerning the electrochemical reduction of sulphate, they found a two-electron reduction to sulphite as shown in Eq. 1.11 which consequently decomposes chemically to sulphide and sulphate as shown in Eq. 1.12.



In the late 1970s, aluminium electrolysis cell was equipped with dry scrubbing system. The main advantage of dry scrubber is to collect and recycle the fluoride material back to the process. Primary  $Al_2O_3$  floating through the dry scrubber acts as sorbent for the removal of gaseous and particulate fluorides from anode

gases with an efficiency of about 99% [1]. The enriched secondary  $\text{Al}_2\text{O}_3$  is then used as feed material. However, dry scrubber brings some disadvantages. The level of impurities after their installation is increased in the metal and in the electrolyte when they are collected and recycled together with the fluorides. This explanation is as show in Table 1.4. Therefore, these have to lead to reduce the current efficiency and decrease the final metal quality.

**Table 1.4:** Impurities concentration and the increase in metal contamination caused by dry scrubber [10]

<b>Impurity source (ppm)</b>	<b>Fe</b>	<b>V</b>	<b>Ni</b>	<b>Cu</b>	<b>Ga</b>	<b>Pb</b>
Fresh $\text{Al}_2\text{O}_3$	80	30	22	72	50	13
Dry Scrubber $\text{Al}_2\text{O}_3$	500	105	250	160	60	70
Anodes	600	140				
Bath	40	10	5	25	7	6
Metal with Dry Scrubber	860	95	44	55	85	42
Metal without Dry Scrubber	500	52	14	28	62	20
<b>Increase due to Dry Scrubber</b>	<b>360</b>	<b>43</b>	<b>30</b>	<b>27</b>	<b>23</b>	<b>22</b>

In contemporary aluminium smelters, electrostatic precipitators are installed in front of the dry scrubber to eliminate these undesired impurities which are concentrated in the finest fraction of the secondary  $\text{Al}_2\text{O}_3$ . This can help in the reduction of the above stated problems in current efficiency and final metal purity. The above mentioned technique reduces the impurities re-circulation but still do not totally remove them.

### **1.3 Phosphorus as an impurity**

As it has already been discussed in Chapter 1.2, phosphorus acts as an impurity element in aluminium production technology. Impurities in general may affect the electrolysis process in various ways. In the case of phosphorus, two effects are of high importance. It is the reduction of the current efficiency and the negative influence on the properties of produced aluminium metal. In industrial conditions, the real influence of phosphorus on the total current efficiency loss is difficult to quantify. However, the current efficiency reduction by about 1% for each 100 ppm of phosphorus is generally accepted [1]. The literature dealing with the behavior of phosphorus compounds in aluminium electrolysis process will be discussed in more details in Chapter 2.

Besides its effect on the current efficiency, phosphorus also affects the properties of the produced metal. Phosphorus lowers corrosion resistance and increases the brittleness of aluminium. The content of phosphorus in aluminium is highly dependent on its concentration in alumina, used technology and on the operational practices and conditions in a given smelter. In primary aluminium produced in modern smelters equipped with dry scrubber, the concentration of phosphorus is ranging from a few ppms up to 30 ppm [11-14].

## 1.4 Silicon as an impurity

Silicon oxide has lower decomposition potential than alumina. The primary source of silicon in the reduction cell is the alumina, refractory bottom lining and SiC sideling. Silicon is nobler than aluminium and tends to be deposited at the cathode electrochemically according to Eq. 1.10 and Eq. 1.13. Hence, they are responsible for most of the contamination of the produced metal.

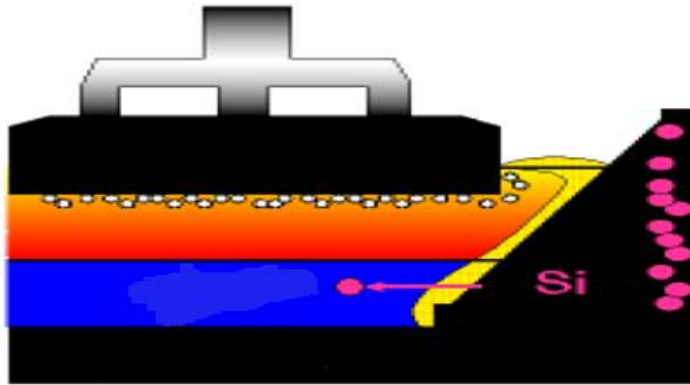


**Figure 1.4:** The amount of silicon on the silicon carbide sideling [2]

For silicon impurity, the maximum concentrations in the final product must be strictly met because of the negative influence on the quality of the final product. Silicon also decreases the current efficiency of the electrolysis process due to the consumption of current which otherwise would be used for aluminium production.

## 1.5 Scope of the work

In the aluminum industry, the current efficiency and metal quality are the most important parameters. Impurities play a detrimental role in the aluminium electrolysis either by being reduced at the cathode and ending up in the metal or by taking part in cyclic red-ox reactions thus consuming electric current and reducing the current efficiency. The impurities of interest in this study are phosphorus and silicon. The objective of the present work is to achieve a common understanding of the behavior of phosphorus and silicon species in the industrial electrolysis cell.

Experiments have been performed in the industrial cells to study the effects of phosphorus and silicon on the current efficiency (%CE) and metal quality. Industrial measurements were carried out by analyzing both bath and metal after addition of phosphorus impurities in the form of  $(\text{AlPO}_4)$  and  $(\text{Na}_3\text{PO}_4)$  to the electrolyte and silicon compound in form of  $(\text{SiO}_2)$ . The concentrations of the element species were measured both in the bath and in the produced metal which were allowed to estimate the equilibrium distribution coefficient (K) for the impurities. Furthermore, measurements were carried by studying the relationship between phosphorus content in the produced aluminium and current efficiency via sodium content in the metal. Copper dilution test was performed to study the changes in metal inventory. The changes in metal inventory between two additions of copper can be used together with tapped metal to find the current efficiency of the cell.

The goal of the work was to study the chemical and electrochemical behavior of phosphorus and silicon impurities in molten cryolite base electrolyte in the industrial cells by determining their transport properties, mass balance and distribution coefficient. This was carried out by monitoring the phosphorus and silicon impurities in the industrial cells before and after external addition of phosphorus and silicon compounds.

## Chapter 2

### 2. Literature review

#### 2.1 General chemistry of phosphorus

In 1669, the alchemist Hennig Brand discovered phosphorus when searching for a way to transform silver into gold. Among several attempts to reach his goal, he dried out a gold colored urine sample by heating it. Afterward, he managed to glow the residue of the urine sample in an oxygen free vessel. By doing so, he obtained a substance. This substance was white phosphorus  $P_5$  which was originally from a phosphorus salt that urine contained. Phosphorus is found in the 5A group of the periodic table of elements. It has a very complex chemistry. Phosphorus is a noble gas configuration which may be reached by means of addition of 3 electrons or by formation of octet of electrons via 4 covalent bonds which means that phosphorus can occur in wide range of oxidation states from  $P^{3-}$  to  $P^{5+}$  [15].

##### 2.1.1 Natural occurrence and production of phosphorus

In the lithosphere, there is about 0.4 atoms of phosphorus for every 100 atoms of silicon where silicon is the second most abundant element in the earth's crust with about 26 wt.% [16]. Also in soils, a variety of phosphates can be found while the phosphorus content of rocks on earth is mostly present in form of apatite. Apatite can also be found in some marine sediment. However, phosphorus found on earth is mainly in its five-valent state. Unlike nitrogen, phosphorus is not found in its elemental state in nature but it is found in form of derivate of phosphoric acid  $H_3PO_4$  because of its high affinity towards oxygen. The production of elemental phosphorus is based on the carbo-thermal reduction of calcium phosphate with silicon oxide at  $1400^\circ\text{C}$ . As shown in Eq. 2.1 besides phosphorus, calcium silicate and carbon monoxide are formed.

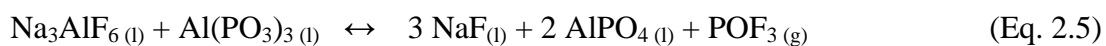


Phosphorus will dime rise upon cooling and form white phosphorus P<sub>4</sub>. Besides white phosphorus, there are other modifications such as red, black and violet phosphorus which are stable under different pressure and temperature conditions. They are differing from each other by structure. When white phosphorus is heated in an oxygen free atmosphere, the substance will melt at 44°C [16]. At its boiling temperature of 280°C, gaseous P<sub>4</sub> molecules will be formed. P<sub>4</sub> molecules will dissociate by 1% into P<sub>2</sub> molecules at 800°C. When reaching 1200°C, about 50% of P<sub>2</sub> will be formed. Above 2000°C, the P<sub>2</sub> molecules will dissociate into P atoms as shown in Eq. 2.2. Therefore at the normal working temperature of 950°C in an alumina reduction cell, any gaseous phosphorus has to be found in the form of P<sub>4</sub> and P<sub>2</sub> molecules.



### 2.1.2 Compounds of phosphorus in the molten state

In recent years, several authors have reported on the stability of different ortho- and meta- phosphates in cryolite based melts. Danek et al. claimed that the phosphorus containing compounds in the solidified melt should be Na<sub>2</sub>P<sub>4</sub>O<sub>7</sub> when mixing cryolite with sodium phosphate, Na<sub>3</sub>PO<sub>4</sub> [17]. When Al(PO<sub>3</sub>)<sub>3</sub> was added to a cryolite melt, the formation of gaseous phosphorus oxy-fluoride, POF<sub>3</sub> occur as shown in Eq. 2.5. The presence of AlPO<sub>4</sub> and POF<sub>3</sub> was confirmed by XRD and IR spectroscopes. In a new publication, the same authors showed by calculation that in the presence of aluminium, compounds of phosphate could be reduced to phosphorus which can either escape as gas or dissolve in the aluminium [18].



Tkatcheva et al. measured the stability of aluminium phosphate, AlPO<sub>4</sub> in a Na<sub>3</sub>AlF<sub>6</sub>-NaF melt with and without added alumina [19]. The results of LECO oxygen analysis and ICP-AES spectroscopy confirmed that AlPO<sub>4</sub> is stable in cryolite based melt. It was found that the ratio between phosphorous and oxygen with and



without presence of alumina is 4. In another publication by the same authors, the stability of the aluminium meta-phosphate,  $\text{Al}(\text{PO}_3)_3$  in cryolite based melt was studied [20]. It was found that the oxygen to phosphorus ratio was stable at 3 throughout the experiment as well as no evolution of  $\text{POF}_3$  gas could be detected. They suggested that the existence of  $\text{PO}_3^-$  as a stable anion in cryolite based melt.

Chaudhuri studied the loss of Al in cryolite based melt when different bath additives and impurities were added [21]. No electrolysis was performed during the experiment. Among several impurities, he also added phosphorus in the form of  $\text{P}_2\text{O}_5$  to cryolite based melt with different alumina contents. It was found that the loss of aluminium increased with increasing amount of phosphorus added to the cryolite based melt. Also, it was found that when more alumina was added, less aluminium was lost.

## 2.2 Phosphorus in industrial aluminium cell

As pointed out earlier in Chapter 1, phosphorus enters the electrolysis cell through the raw materials. Table 2.1 shows examples of phosphorus pent-oxide;  $P_2O_5$  contents in the main raw materials for the aluminium electrolysis process. It seems from Table 2.1 that alumina has the lowest phosphorus content; however, the amount of alumina added per tonne of aluminium produced varies enormously between the different raw materials. For instance, the amount of alumina required to produce one tonne of aluminium is about 2000 kg. For the aluminium fluoride, a maximum of 20 kg per tonne of aluminium is needed. Since the introduction of additional bath is not a routine procedure, the amount of cryolite added per tonne of aluminium is fairly low. It is approximately 10 kg per tonne of aluminium. Table 2.2 shows the distribution of  $P_2O_5$  when the amount of the raw materials added to the industrial aluminium cell per tonne of aluminium produced is considered. It is seen from Table 2.2 that the major amount of phosphorus is originated from the alumina and the amounts of the cryolite and aluminium fluoride added are negligible.

**Table 2.1:** Contents of phosphorus expressed as  $P_2O_5$  in different raw materials in ppm

Alumina, $Al_2O_3$	Aluminium Fluoride, $AlF_3$	Cryolite, $Na_3AlF_6$	Literature source
0.1-0.5	1.6-2.1	0.8-1.3	[22]
0.09	1	-	[23]
0.1-0.3	-	-	[24]

**Table 2.2:** Contents of phosphorus expressed as P<sub>2</sub>O<sub>5</sub> in different raw materials per tonne of aluminium produced in ppm

Alumina, Al <sub>2</sub> O <sub>3</sub>	Aluminium Fluoride, AlF <sub>3</sub>	Cryolite, Na <sub>3</sub> AlF <sub>6</sub>	Literature source
20-100	3.2-4.2	0.8-1.3	[22]
18	2	-	[23]
20-60	-	-	[24]

It is important to study the production of the cryolite and aluminium fluoride to distinguish why the level of phosphorus is higher than in alumina. The relatively high contents of phosphorus in Na<sub>3</sub>AlF<sub>6</sub> and AlF<sub>3</sub> originate from hydrogen fluoride, HF which is utilized to produce them. It is advantageous for economic reason to use HF from super-phosphate production where it occurs as a by-product [22]. Eq. 2.11, Eq. 2.12 and Eq. 2.13 show the involved reactions in the production of cryolite. Since sodium fluoride, NaF and cryolite, Na<sub>3</sub>AlF<sub>6</sub> have a low solubility in aqueous solutions, they will precipitate and consequently are removed. Grjotheim stated that it is challenging to keep the phosphorus content in the cryolite below a certain limit as required by the aluminium smelters [4].



The reaction of a slurry of aluminium hydroxide, Al(OH)<sub>3</sub> with hydrogen fluoride, HF gas is used to produce aluminium fluoride, AlF<sub>3</sub> in the process called wet fume scrubbing. This reaction is shown in Eq. 2.14. The

hydrogen fluoride for the production of  $\text{AlF}_3$  normally originates from super-phosphate manufacturing. Thus,  $\text{AlF}_3$  is more contaminated with phosphorus than  $\text{Al}_2\text{O}_3$ .



As well, the production of  $\text{Al}_2\text{O}_3$  from bauxite by the Bayer process generates phosphorus impurity but to a much lower extent than for  $\text{Na}_3\text{AlF}_6$  and  $\text{AlF}_3$ . In bauxite deposits, the hydrated alumina is always associated with little impurities which flow through the alumina production process and end up in it to a minor extent [22]. For other additives to the industrial electrolysis cell such as  $\text{CaF}_2$ ,  $\text{LiF}$ ,  $\text{NaF}$  and  $\text{MgF}_2$ , it was found no specifications on phosphorus contents. Since small amounts of these substances are added to the electrolysis cells, their contribution to the phosphorus content in the cell is negligible. Moreover, some phosphorus is present in the carbon anode. Industrial figures showed an average concentration of 7 ppm phosphorus in the anode but this may vary along with the quality of raw materials used for anode production [25]. Since the carbon is electrochemically oxidized, any impurity will go through the electrolyte or form volatile compounds and evaporate with the anode gases.

### 2.2.1 Laboratory studies

In this chapter, previous laboratory analysis of phosphorus behavior in aluminium electrolysis process is reviewed. Deininger and Gerlach studied effect of phosphorus in the form of  $\text{P}_2\text{O}_5$  on current efficiency of aluminium electrolysis in laboratory reduction cell [26]. They stated that the phosphorus electrochemical behavior in the studied system depends on its concentration. At phosphorus concentration up to 1200 ppm, they suggested two-electron cyclic red-ox reaction as shown in Eq. 2.15. This is found to be responsible for the measured current efficiency losses (95% per 100 ppm of phosphorus). Whereas at phosphorus concentration higher than 1200 ppm (unlikely in the real industrial conditions), the five-electron cyclic red-

ox reaction should be the dominant electrochemical reaction of phosphorus as shown in Eq. 2.16. They as well observed formation of elementary phosphorus at phosphorus concentration above 1500 ppm.

Additional noticeable feature was the increase of cell voltage with phosphorus concentration.



Qiu et al. studied the distribution of Ni, Ga, Fe, Si, P, V and Ti between metal and bath in a laboratory electrolysis cell [27]. They determined equilibrium distribution coefficient,  $K$  for the impurities as shown in Eq. 2.17. Higher value of equilibrium distribution coefficient,  $K$  indicates weaker tendency to be reduced into the metal at the cathode. The experimental electrolysis system consisted of graphite anode, aluminium cathode and cryolite melt containing the dissolved impurities. The impurities were blended into the bath mixture before the experiment. The experiment was carried out at 2 different conditions. One was without electrolysis and the other was with electrolysis. In the first case, the electrolysis cell was heated for 4 hours and the impurities were just reduced chemically by Al metal. While in the second case, 4 hours electrolysis was performed. Distribution of the impurities between bath and metal was determined in the both cases. The equilibrium distribution coefficient,  $K$  value depends on the impurity concentration in the melt. During the experiment, 4 different impurity levels were checked.

$$K = \frac{\text{impurity content in bath (ppm)}}{\text{impurity content in Al metal (ppm)}} \quad (\text{Eq. 2.17})$$

It was found that phosphorus has the highest equilibrium distribution coefficient,  $K$  compared to the other elements for both chemical and electrochemical reduction as illustrated in Table 2.3 in Appendix A [27]. It

means that phosphorus has a higher tendency to remain in the bath than the other studied elements. In addition to the impurities given in the table below, the distribution coefficient for Ni, Ga, V and Ti were determined. Also, the distribution coefficient for phosphorus in the laboratory reduction cell was found to be close to or equal to 1 which is very different from the distribution coefficient found for industrial cells. The distribution coefficient for phosphorus in industrial cells is expected to be 6.2 [28]. However, it needs to be highlighted that Sturm and Wedde had a dry scrubber unit involved in the system which captured the volatile phosphorus compounds and thus the amount of phosphorus in the secondary alumina is increased [28].

Solli studied the changes in current efficiency by adding various impurities to a laboratory electrolysis cell and he showed that an addition of 0.01 wt.% of phosphorus reduced the current efficiency by 0.68% [29]. The phosphorus was added in the form of  $P_2O_5$  and  $Ca_3(PO_4)_2$ . The current efficiency value attained was a slight lower than that usually obtained in the industrial cells. As specified in Chapter 1, for every 100 ppm phosphorous in the bath of the industrial cell, the current efficiency is reduced by about 1%.

Custhall studied the distribution of phosphorus impurity between size fractions of secondary alumina and a possibility of phosphorus removal from secondary oxide [30]. Table 2.4 presents the results of size and concentration analysis of dry scrubber alumina. The tabulated figures show that the phosphorus concentration increases with decreasing size of particles due to their higher surface area. In the finest fraction, the concentration of phosphorus is almost six times higher than that in the whole bulk. It is found that the optimum method to reduce the impurity content in secondary oxide is by separation of fines from secondary alumina. This approach causes loss of significant amounts of alumina and fluorides. For instance, separation of particles, 325 meshes causes a loss of 15% of alumina while the phosphorus content is reduced just around 50% [30].

**Table 2.4:** Size and phosphorus concentration analysis of secondary alumina [30]

<b>Size fraction (<math>\mu\text{m}</math>)</b>	<b>Weight fraction (%)</b>	<b>Phosphorus concentration (ppm)</b>	<b>Fraction of total phosphorus (%)</b>
+150	5.4	13	1.5
74-150	56.8	22	26.6
43-74	23.4	35	17.5
38-43	7.2	61	9.2
38	7.2	297	45.2
Composite	100	48	100

Custhall found that flotation of the secondary alumina enables the reduction of phosphorus content to not less than 80% [30]. Lossius and Øye tested several ways of purification for secondary oxide fines [31]. They treated 2% fines stream of secondary alumina containing 50% of impurities. The most favorable method is the fines wet fractionation (settling) combined with magnetic separation [31]. In general, the laboratory studies of phosphorus in aluminium electrolysis relate mostly to its effect on the current efficiency and to the reduction of the impurity content in the secondary alumina.

### 2.2.2 Industrial studies

Danek et al. carried out a material balance in SLOVALCO smelter (aluminium plant in Slovakia). They followed the phosphorus concentration in consumed and produced materials over 3 years from year 1997 to 1999 [14]. This smelter is equipped with modern prebaked HAL 230 cells and dry scrubbers. Since the SLOVALCO smelter was during the time a plant, very pure metal was produced at the beginning of the following period. However over the following three years, the content of phosphorus increased considerably in the produced aluminium metal as well as in the bath. The phosphorus concentration ratio (bath/metal) was 10.3 in 1999 [14]. The secondary  $\text{Al}_2\text{O}_3$  contained about 5 times more phosphorus than the primary  $\text{Al}_2\text{O}_3$ . This increase of the phosphorus concentration in the covering material points out that condensation or solid species trapping occur. Considering the entire smelter as a balanced system, splitting of phosphorus between outgoing streams is as follows. 61% is in metal, 21% is in discharging anode cover, 14% is in gas emissions and 4% is in anode butts [14]. It was assumed that 95% of phosphorus from the anode gas is trapped to the secondary  $\text{Al}_2\text{O}_3$  while the rest 5% escapes through the dry scrubber to the atmosphere. The results of the three years mass balance accomplished by Danek et al. in SLOVALCO smelter are summarized in Table 2.5, Table 2.6 and Table 2.7 in Appendix A.

Thisted carried out a mass balance of phosphorus for a Soderberg line in Hydro Aluminium ARDAL smelter (aluminium plant in Norway) [11]. The electrolyte cells are fed with pure primary  $\text{Al}_2\text{O}_3$ . Here, the dry scrubber is not included in the illustrated mass balance. When compared to the prebaked cells in the same smelter accomplished by Haugland et al. [32], it was found that the Soderberg line operates with a lower acidity, 9-10 wt.% excess  $\text{AlF}_3$  while the prebaked cells have an acidity of 12-13 wt.%. Also, the Soderberg line operates with a higher temperature, 965-970°C whereas the prebaked cells have a temperature of 960-963°C. The results of the phosphorus mass balance done by Thisted are demonstrated in Table 2.8 in Appendix A. Most of the phosphorus leaves the Soderberg cells as the gas around 70%, 18% as solid dust and 12% in aluminium metal [11]. The bath-metal ratio was found to be 27.5 which are considered very high.



Haugland et al. performed a mass balance of phosphorus for prebaked cells in Hydro Aluminium ARDAL smelter (aluminium plant in Norway) [32]. The cells were fed by secondary  $\text{Al}_2\text{O}_3$ . They concluded that 80% of the entering phosphorus was turned out in the final aluminium metal. In addition, they studied effect of several process parameters on the phosphorus content in the metal produced. A number of findings were detected. The most significant one was that high temperature causes more phosphorus transfer from bath to gas phase; therefore, the phosphorus concentration in the produced aluminium is low. Also after the anode effect, the phosphorus concentration in the aluminium is reduced. This may be due to the high temperature during the anode effect. Additionally in newly started cell, low phosphorus concentration in the aluminium is generally found. It may be because of its high operating temperature or different bath chemistry of new cell.

Cutshall carried out further work on how to remove phosphorus from secondary  $\text{Al}_2\text{O}_3$  [30]. He investigated various techniques for purifying secondary  $\text{Al}_2\text{O}_3$  from phosphorus. It was found that flotation is the most advantageous and practical technique. By using this method, the phosphorus level in the secondary  $\text{Al}_2\text{O}_3$  was lowered by 80%. He pointed out that a high phosphorus level in the electrolyte cell leads to a higher operating temperature and therefore reduced the current efficiency.

Thisted studied the transport of phosphorus which was added as  $\text{Na}_3\text{PO}_4$  from bath to metal in industrial prebaked cells in Hydro Aluminium ARDAL smelter in Norway [11]. In this study, phosphate was added to the bath and the phosphorus concentration was observed. It was found that the phosphorus concentration decrease in bath is much slower than when metals such as silicon or titanium are added. Also, the built up concentration of phosphorus in metal is lower than the concentration of instantaneously added metals. In addition, she tested the effect of anode cathode distance (ACD) on phosphorus distribution [11]. During this test, the ACD was reduced by 1 cm for 2 hours; consequently, it was found that there was a decrease in phosphorus concentration in bath and metal. This occurred due to the changed transfer conditions in the system as lowering the ACD will cause more intensive bath mixing as explained by Thisted [11]. This leads to depression of the bath/metal diffusion layer and, therefore, to hasten the transport of reduced impurities

such as phosphorus from the cathode back to the bath. The decrease in bath concentration is because of hastened transport of carbon species with adsorbed impurities from the bath to the gas phase.

Oblakowski and Pietrzyk investigated several industrial bath samples. They found a linear relationship between the carbon and the phosphorus content in the bath [33]. They concluded that increased contents of phosphorus and carbon in form of C and  $Al_4C_3$  in the bath are the reasons for an increased operating temperature of the industrial cell. The relationship between carbon and phosphorus was explained by the increased wet-ability of the carbon particles by the bath in the presence of phosphorus. This makes it more difficult for the carbon to reach the bath surface and be oxidized to  $CO_2$ .

Bomh et al. studied the removal of impurities from a gas phase in the aluminium smelter by using dry scrubber. They carried out a mass balance of impurities in 3 electrolyte cells [34]. It was found that 72% of the entering phosphorus leaves the cell in the gas phase, 12% accumulated in the metal and the rest possibly in the bath. They also studied the efficiency of an electrostatic separator associated with the cells and the dry scrubber. It was found that the electrostatic separator reduced the impurities content in the gas phase by 90%. The separation of secondary  $Al_2O_3$  was smaller than 1  $\mu m$  provided impurity removal is in the range of 50-70%.

Augood reviewed literature experimental data relating to the impurities distribution within the streams entering and existing the electrolyte cell (feed, metal and gas) [35]. He calculated equilibrium constants for an impurity distribution between gas/feed and gas/metal streams. For phosphorus, it was proposed to be 0.91 for gas/feed stream and 10 for gas/metal stream [35]. It corresponded to the fact that 90% of incoming phosphorus leaves the cell in the gas phase and evidently the amount of phosphorus in the gas is roughly 10 times higher than in the metal. It has to be noted that these values are just corresponded to an electrolyte cell without dry scrubber unit installation. When this cell is installed with dry scrubber, the resulting values are significantly different due to recycling of impurities back to the cell by the secondary  $Al_2O_3$ .

An industrial report by Handa showed that the quality of alumina when compared with phosphorus is significant for having an optimal production of aluminium [36]. He stated that the normal phosphorus content in primary  $\text{Al}_2\text{O}_3$  used at the KUBAL smelter (aluminium plant in Sweden) was lower than or maximum 10 ppm over last two decades before it increased [36]. It can be seen from Table 2.9 that different primary  $\text{Al}_2\text{O}_3$  shipments showed different phosphorus content. Due to operational problems at the KUBAL smelter and a decrease in current efficiency in the prebaked cells, all standard practices and parameters were checked. It was found that the phosphorus content in the electrolyte was increased from 43 ppm to 126 ppm. The fact that 100 ppm of phosphorus in the bath decreases the current efficiency by 1% was verified since the increase of phosphorus content by 83 ppm decreased the current efficiency by 0.8% at the KUBAL smelter.

**Table 2.9:** Primary alumina shipments from different suppliers and their phosphorus contents [36]

Type of $\text{Al}_2\text{O}_3$ (Date of arrival)	Phosphorus content (ppm)
Alumina A1 (07/06/1999)	14
Alumina A2 (17/01/2000)	17
Alumina A3 (31/03/2000)	28
Alumina A4 (18/05/2000)	19

As phosphorus mostly originates from the alumina added to the electrolyte cell, several authors have attempted to estimate a satisfactory concentration limit of phosphorus in alumina. Richards proposed that the phosphorus content in  $\text{Al}_2\text{O}_3$  should be lower than 0.001 wt.% for use in aluminium production smelter [24]. Grjotheim and Welch supported the recommendation as showed by Richards [22]. Homsy suggested slightly higher phosphorus content up to 0.0012 wt.% to be utilized in aluminium plants [37].

Much attention was paid to distribution and behavior of phosphorus concentration in the industrial Hall-Hèroult cell. Dry scrubber and ultimately fines separation extremely influence the phosphorus distribution. In

smelter without dry scrubber unit installation, the majority of the phosphorus leaves the electrolysis cell in the gas phase. Although smelters with dry scrubber, most of the phosphorus around 80% end up in the produced metal. The separation of secondary  $\text{Al}_2\text{O}_3$  fines with enhanced impurity levels such as for phosphorus will possibly provide essential improvement in metal quality and current efficiency.

## 2.3 General chemistry of silicon

The atomic number of silicon is 14, while its symbol is Si. It belongs to the group of tetravalent metalloids in the periodic table. The group contains other elements like carbon, but silicon exhibits different chemical behavior as compared to other group members. Silicon is solid at room temperature. It has a comparatively high conductivity for heat,  $149 \text{ W}\cdot\text{m}^{-1}\cdot\text{K}^{-1}$ , and therefore it has good heat conductivity [38]. The outer ring of silicon's atoms has four electrons like carbon.

### 2.3.1 Natural occurrence and production of silicon

Silicon comes second in terms of natural occurrence on the crust of the earth. It is estimated that the crust of the earth is 27.6 percent silicon [38]. The element therefore comes second after oxygen as the most abundant element on the crust of the earth. It is believed by some authorities that rocks made of oxygen and silicon compounds account for more than 97% of the crust of the earth [38]. It is important to note at this point that silicon cannot be found occurring freely in nature. Silicon is always found as part of compounds with other elements like phosphorous, magnesium, calcium, oxygen and other elements. Silicon is more common in compounds that have some form of silicon dioxide, which are referred to as silicates. Scientists have detected silicon in stars and the sun, and it is believed that silicon forms part of some meteorites.

By the early 1800s, scientists recognized silicon as an element [38]. It was however a challenge preparing pure silicon because the element has a high affinity for oxygen and thus it bonds to the latter tightly. It took a number of years for scientists to devise a way of separating oxygen and silicon. The separation of the two was accomplished by Jons Jakob Berzelius, a Swedish chemist in the year 1823 [38]. The commercial preparation of silicon is done by a reaction that involves highly-pure silica, coal, charcoal, and wood, which is done using carbon electrodes in an electric-arc furnace. Eq. 2.18 shows the chemical reaction that silicon undergoes at temperatures exceeding  $1,900^\circ\text{C}$  [38]. After the reaction, liquid silicon forms and moves to the

furnace's bottom, after which it is drained and cooled. This method produces 98 percent pure silicon that is referred to as metallurgical grade silicon.



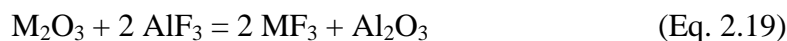
### 2.3.2 Silicon alloys

There is a rapid increase in the use of aluminium-silicon alloys mainly in the automobile industry because of their high strength to weight ratio, high wear resistance, low density and low coefficient of thermal expansion [38]. High silicon content alloyed into aluminium adds a huge amount of heat capacity which has to be eliminated from the alloy to solidify it throughout the casting operation. Consequently, it causes major deviation in the mechanical properties. In addition, the strength properties of Al-Si alloys reduce with additional increase in the silicon content.

One of silicon's alloys is ferrosilicon, which has different ratios of iron and elemental silicon. Ferrosilicon is responsible for almost 80 percent of the elemental silicon that is produced all over the world [38]. The leading supplier of this silicon world over is China. The alloy ferrosilicon is applied primarily in the steel industry. Silumin alloys, which are made up of silicon and aluminium find their most applications in the industry that casts aluminium alloys. In that industry, silicon is highly valued because it leads to better casting properties for aluminium. Silumin alloys are high-strength and lightweight, and they have a silicon content of between 3 percent and 50 percent [38]. Most of the alloys are casted. One of the alloys, 6061, has silicon and magnesium as its major elements for alloying. It was first developed in the year 1935, and its original name was Alloy 61S [38]. It has valuable properties including the fact that it has good weld-ability and its mechanical properties are good. 6061 alloy is among the commonest aluminium alloys that are used for general purposes. Cast aluminium finds great use in the manufacture of automobiles and thus silicon use in this industry is actually the largest industrial use of pure silicon of metallurgical grade.

## 2.4 Silicon in industrial aluminium cell

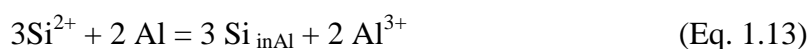
Industrial Hall-Héroult cells always contain impurities, with silicon being among the major impurities. The raw materials bring the impurities and they are continually added by carbon anodes, silicon carbide sideling and alumina feeding. The alumina is the main source of silicon as an impurity in this case. The impurities become part of the process because of the dissolution of metal oxides as shown in Eq. 2.19.



There are a number of reasons for investigating the behavior of silicon impurities in the industrial Hall-Héroult cells. However, this study considers three reasons as outlined below:

- ❖ They negatively affect current efficiency (%CE).
- ❖ Most aluminium contamination is caused by silicon impurities.
- ❖ The bath continuously has increased concentrations of impurities because dry scrubbers are used in the process.

The silicon impurity that is present in the bath leads to contamination of the produced aluminium metal since the impurity's oxide does not have a decomposition potential that is as high as that of alumina. At the cathode, the metal oxide undergoes electrochemical reduction according to Eq. 1.13.



Some of the silicon impurities are lost together with the exit gas, a process that is believed to be as a result of the volatility of  $\text{SiF}_4$ .  $\text{SiF}_4$  is normally formed in this process by an anode reaction or by a reaction in the bath according to Eq. 2.20.



## Chapter 3

### 3. Theory

Metallic impurities such as silicon behave differently from non-metallic impurities such as phosphorus. Studies of mass transfer of metallic impurities by Jentoftsen [5] showed that these impurities mainly accumulate in the metal as expected since they are nobler than aluminium. The mass transport between bath and metal in the electrolysis cell occurs continuously where generally a species  $M^{n+}$  that is nobler than aluminium can be transferred electrochemically to the metal. The electrochemical reaction at the cathode is able to be divided into a number of stages as shown in Figure 3.1. The steps are:

- i. Transport of species  $M^{n+}$  through the boundary layer between bath and metal.
- ii. Reduction of  $M^{n+}$  to  $M$  at the interface.
- iii. Further transport of  $M$  from the interface into the metal.

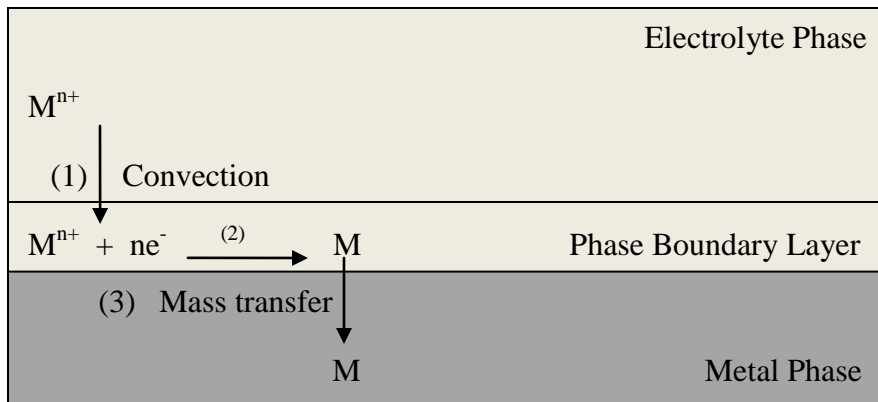


**Figure 3.1:** Mass transport of species  $M^{n+}$  from the electrolyte into the produced aluminium

Based on this mechanism, impurities are deposited at the cathode and its limiting current density ( $i_l$ ) relies on the concentration of the element in the electrolyte ( $c^0$ ) and on the mass transfer coefficient ( $k_m$ ).



$$i_l = n \times F \times k_m \times c^0 \quad (\text{Eq. 3.1})$$

Assuming that step 1 in Figure 3.1 controls the mass transfer process, the flux of a species transferred from the bulk to the electrolyte/metal interface can be expressed as:

$$J = A \times k \times (c_{\text{bath}} - c_{\text{boundary}}) \quad (\text{Eq. 3.2})$$

If step 2 and 3 in Figure 3.1 are comparably faster than step 1,  $c_{\text{boundary}}$  can be assumed to be equal to zero. Thereby, the expression for the flux in Eq. 3.2 will be simplified.

$$J = A \times k \times c_{\text{bath}} \quad (\text{Eq. 3.3})$$

The flux also can be expressed as a partial current.

$$I = n \times F \times J = n \times F \times A \times k \times c_{\text{bath}} \quad (\text{Eq. 3.4})$$

Thus, the change of concentration in the bath as a function of time is stated as:

$$J = -V \times \frac{dc}{dt} = A \times k_{\text{bath}} \times c_{\text{bath}} \quad (\text{Eq. 3.5})$$

Integration of Eq. 3.5 results in:

$$c_{\text{bath}}(t) = c_{\text{added}} \times \exp(-A \times V^{-1} \times k_{\text{bath}} \times t) \quad (\text{Eq. 3.6})$$

$c_{\text{bath}}$  can either be expressed as the amount of impurity added or the variation between the concentration in the bath instantaneously after addition and the background concentration  $c_{\text{bc}}$  which fundamentally should be the same if the addition is complete. It is meant that the impurities added to the reduction cell are completely dissolved in the electrolyte and there are no losses due to the environment. Thus, Eq. 3.6 can be expressed as:

$$c_{\text{bath}}(t) = c_{\text{bc}} + c_{\text{added}} \times \exp(-A \times V^{-1} \times k_{\text{bath}} \times t) \quad (\text{Eq. 3.7})$$

Mass transfer coefficients were calculated by Jentoftsen [5] for iron, titanium and silicon and turned out to be  $(10\pm 3) \cdot 10^{-6}$  m/s,  $(7\pm 3) \cdot 10^{-6}$  m/s and  $(5\pm 2) \cdot 10^{-6}$  m/s respectively.

Studies of impurity species in industrial Hall-Héroult cell are accomplished by analyzing samples of bath and metal over time after adding of a certain amount of impurity compounds. The concentration of the impurities against time after addition is stated as follows:

$$c = c_o \exp\left(-\frac{A}{V} kt\right) \quad (\text{Eq. 3.8})$$

Thus, the mass transfer coefficient is capable of being found out from the above demonstrated relationship. Mass transfer coefficients mainly rely on design, technology and operation of industrial electrolysis cells. High convection of bath and metal pad or unstable cell is the main reason of higher value of mass transfer coefficient.

### **Metal inventory by copper dilution:**

By adding a certain amount of copper and analyzing copper content of aluminium in the cell before and after copper is added, it is possible to calculate metal reservoir. Changes in metal reservoir between two additions of copper can be used together with tapped metal to find the current efficiency of cells. The metal reservoir is calculated using Eq. 3.9:

$$\text{Metal reservoir} = [C_{\text{Cu}} \times M_{\text{Cu}}] / [1000 \times (C_2 - C_1)] \quad (\text{Eq. 3.9})$$

## Chapter 4

### 4. Experiment

Experiment was performed with respect to phosphorus and silicon in industrial cells. Bath and metal samples were analyzed as a function of time after adding a certain amount of tri-sodium phosphate ( $\text{Na}_3\text{PO}_4$ ), aluminium phosphate ( $\text{AlPO}_4$ ) and silicon dioxide ( $\text{SiO}_2$ ). Several process variables such as temperature were studied in connection with the concentration of phosphorus and silicon in the electrolytic cell. Trends in phosphorus and silicon content in aluminium produced in industrial cells were also studied from analytical data. The procedures for adding the impurity species to the electrolyte were as the following. Initially, the crust was fractured. Next, the impurity species were cautiously added to the electrolyte. All the time, the insertion of impurities was made in the tapping hole. However, the addition was placed at some further positions to improve the allocation of the impurities.



**Figure 4.1:** A certain amount of  $\text{Na}_3\text{PO}_4$ ,  $\text{AlPO}_4$  and  $\text{SiO}_2$  were added in the industrial cells

Since the major part of the phosphorus impurity enters the process with alumina addition in its highest oxidation state, phosphorus was added in the five valent form as  $\text{AlPO}_4$  and  $\text{Na}_3\text{PO}_4$ , while the silicon was added as  $\text{SiO}_2$ . All measurements were performed at Qatar Aluminium Company (QATALUM). Samples were taken from bath and metal at regular intervals for analyzing before and during the experiment. The

samples were marked and placed in proper place. Bath samples were analyzed by X-ray Fluorescence (XRF). Metal samples were analyzed by automated optical emission spectroscopy (OES).



**Figure 4.2:** Bath and metal samples were taken and placed in proper place in able to be analyzed

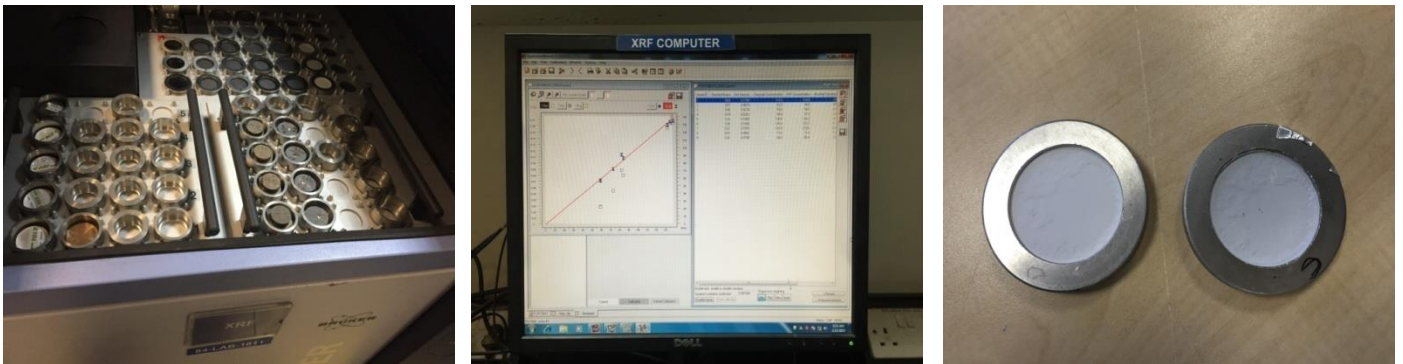


**Figure 4.3:** Bath samples were analyzed by X-ray Fluorescence (XRF)



**Figure 4.4:** Metal samples were analyzed by automated optical emission spectroscopy (OES)

Also, a certain amount of copper was added and subsequently the copper content in aluminium in the electrolyte cell was analyzed before and after the copper was added. Thus, the metal reservoir also called metal inventory could be calculated. Changes in the metal reservoir between two additions of copper can be used together with tapped metal to find the current efficiency of the cell.

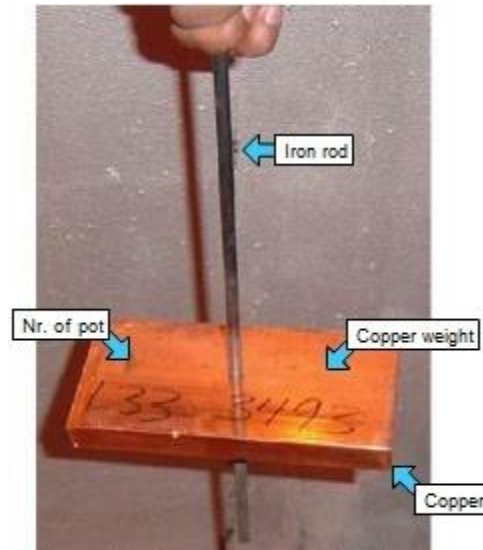


**Figure 4.5:** Metal inventory by copper dilution

The cell type used for the experiments was side-by-side prebake cell which have 30 anodes and 5 feeders. These cells are operated at 300-350 kA. This cell is fed by secondary alumina and the aluminium produced is tapped once a day. 3 cells were used for this particular experiment. These cells were chosen based on specific criteria. The selection criteria of the chosen cells are:

- ❖ Reference Cells (Having History in Metal Inventory)
- ❖ Stability (Good in Thermal balance and Noise)
- ❖ Quality (Low impurities content)



**Figure 4.6:** QATALUM side-by-side prebake cells with 30 anodes

## Chapter 5

### 5. Results and Discussion

#### 5.1 Distribution of phosphorus and silicon after addition

A number of measurements were achieved in QATALUM cells where phosphorus compounds in form of  $(\text{AlPO}_4)$  and  $(\text{Na}_3\text{PO}_4)$  to the electrolyte and silicon compound in form of  $(\text{SiO}_2)$ . Samples were taken from the bath and from the metal for analysis.

Figure 5.1 and Figure 5.2 show the concentration of phosphorus in the bath and in the metal as a function of time before and after adding aluminium phosphate  $(\text{AlPO}_4)$ . However, Figure 5.3 and Figure 5.4 show the concentration of phosphorus in the bath and in the metal as a function of time before and after adding tri-sodium phosphate  $(\text{Na}_3\text{PO}_4)$ . To compare the behavior of phosphorus to that of metallic impurities, results for silicon are shown also shown. Figure 5.5 and Figure 5.6 show the concentration of silicon in the bath and in the metal as a function of time before and after adding silicon dioxide  $(\text{SiO}_2)$ .

It can be seen that phosphorus has a much longer retention time in the bath than silicon. Also, it is apparent in the case of silicon that the decrease in the bath leads to an increase in the metal, the concentration of phosphorus in the bath seems to reduce far more slowly. The increase in the metal is almost immediate after addition and the concentration remains more or less constant during the time of the measurement. A feasible reason is that phosphorus gas is produced at the cathode. Most of them leave the cathode and are oxidized in the bath. This process could be repeated few times which makes a longer residence time in the bath and therefore a negative effect on the current efficiency. This shows that even though phosphorus is more electropositive element than aluminium, the main part of it was found to remain in the bath.

### P in Bath (in PPM) after addition of $\text{AlPO}_4$

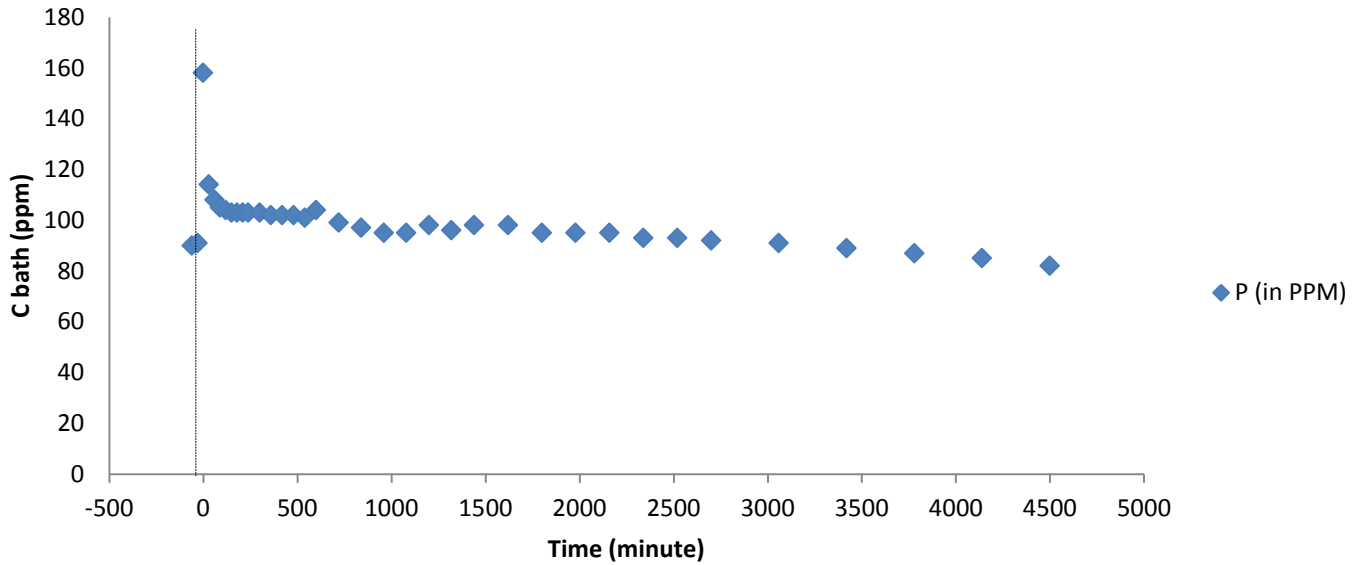


**Figure 5.1:** Distribution of phosphorus in the bath as a function of time after adding  $\text{AlPO}_4$ . The dotted line marks the time of addition

### P in Metal (in PPM) after addition of $\text{AlPO}_4$

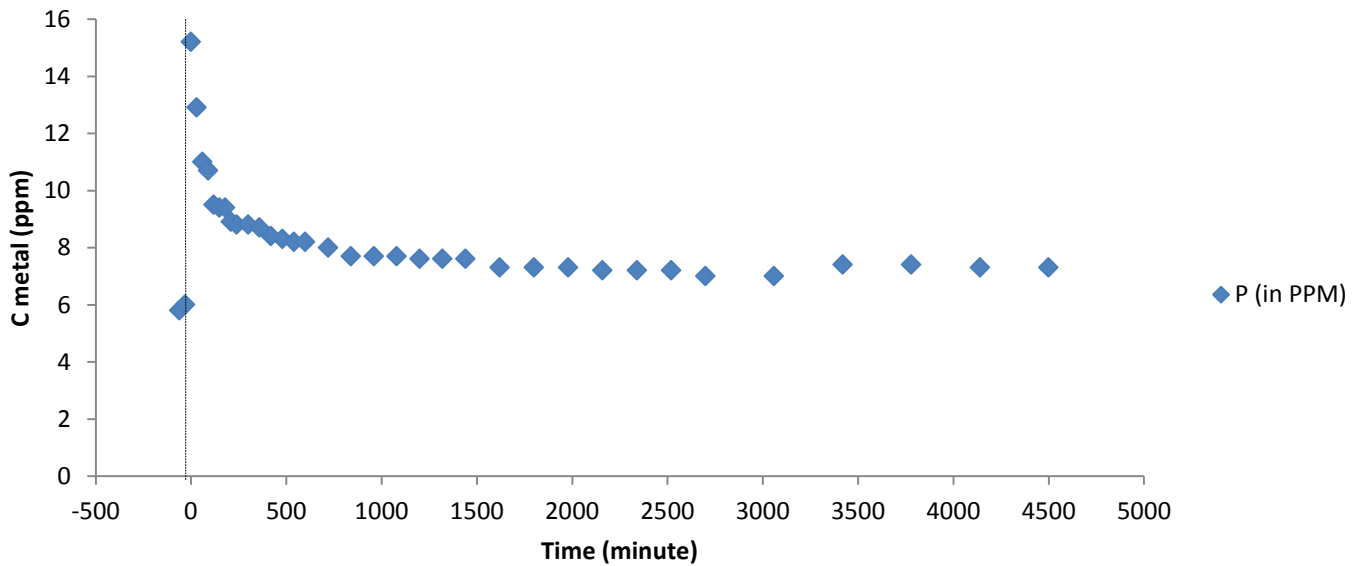


**Figure 5.2:** Distribution of phosphorus in the metal as a function of time after adding  $\text{AlPO}_4$ . The dotted line marks the time of addition



### P in Bath (in PPM) after addition of $\text{Na}_3\text{PO}_4$

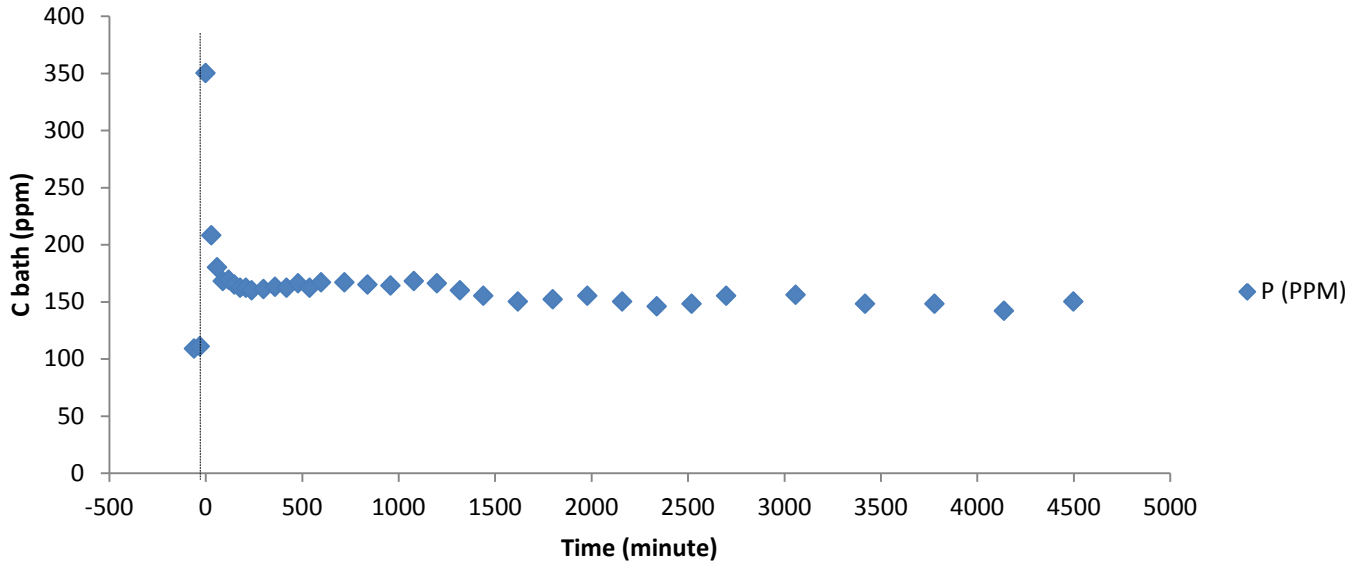


**Figure 5.3:** Distribution of phosphorus in the bath as a function of time after adding  $\text{Na}_3\text{PO}_4$ . The dotted line marks the time of addition

### P in Metal (in PPM) after addition of $\text{Na}_3\text{PO}_4$

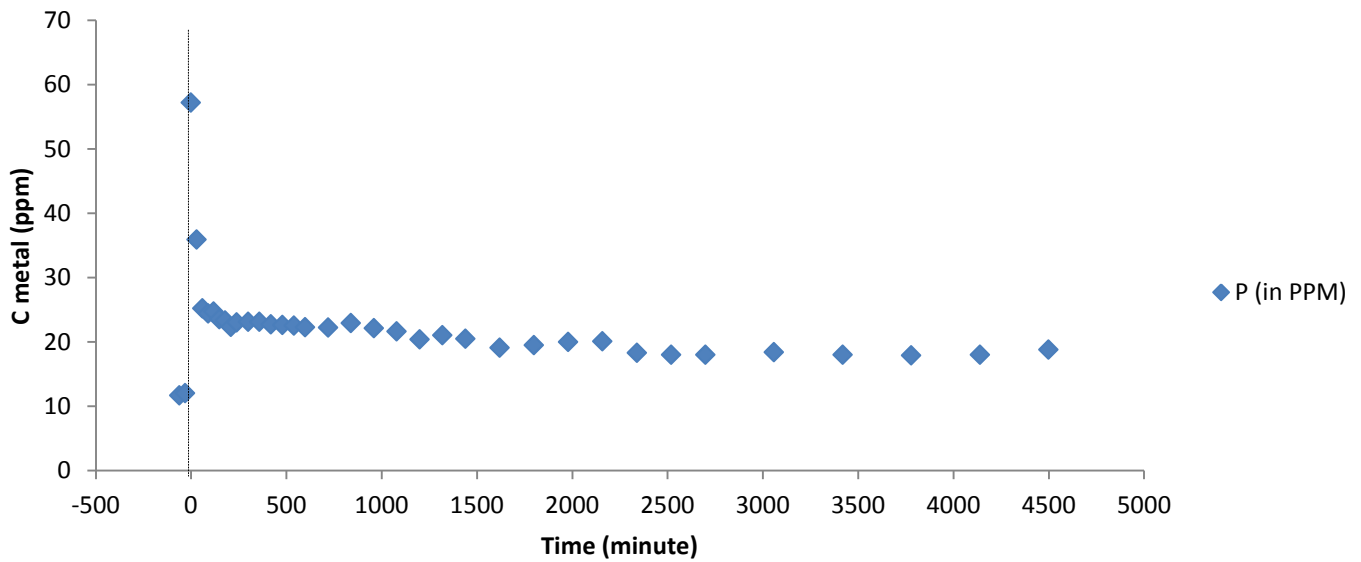


**Figure 5.4:** Distribution of phosphorus in the metal as a function of time after adding  $\text{Na}_3\text{PO}_4$ . The dotted line marks the time of addition

### Si in Bath (in PPM) after addition of SiO<sub>2</sub>

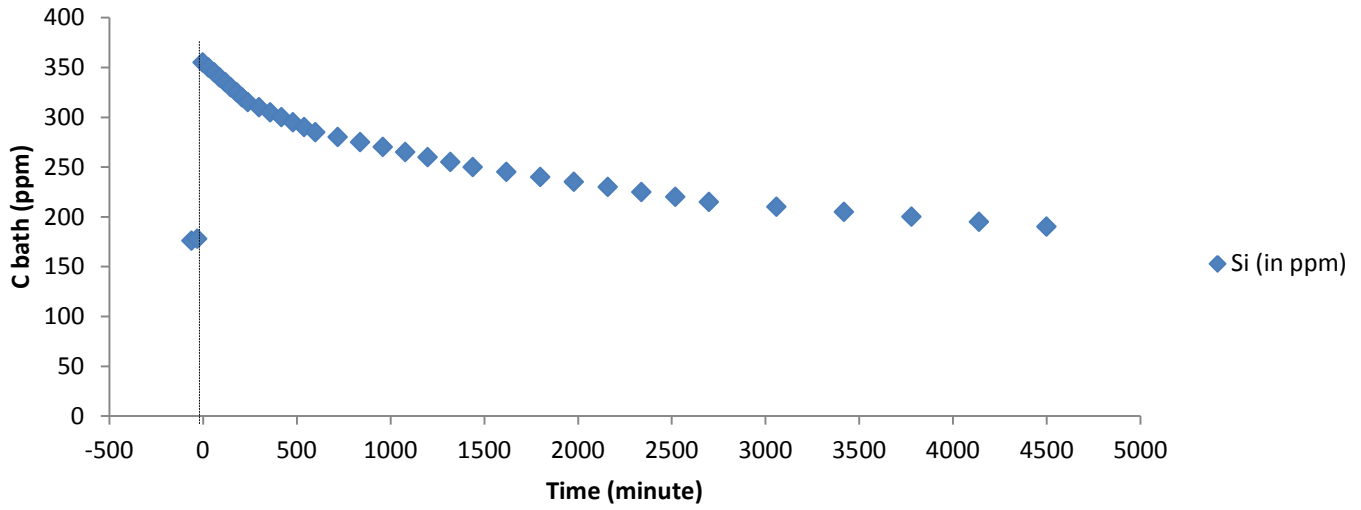


**Figure 5.5:** Distribution of silicon in the bath as a function of time after adding SiO<sub>2</sub>. The dotted line marks the time of addition

### Si in Metal (in PPM) after addition of SiO<sub>2</sub>

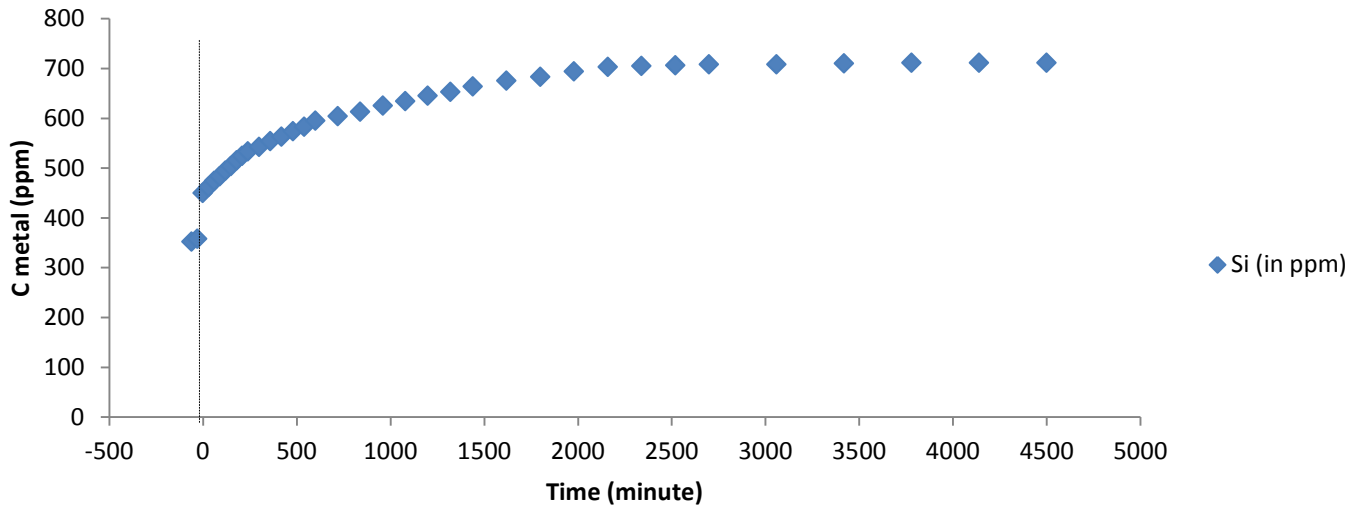


**Figure 5.6:** Distribution of silicon in the metal as a function of time after adding SiO<sub>2</sub>. The dotted line marks the time of addition

### P and Si in Bath after addition of $\text{AlPO}_4$ , $\text{Na}_3\text{PO}_4$ and $\text{SiO}_2$

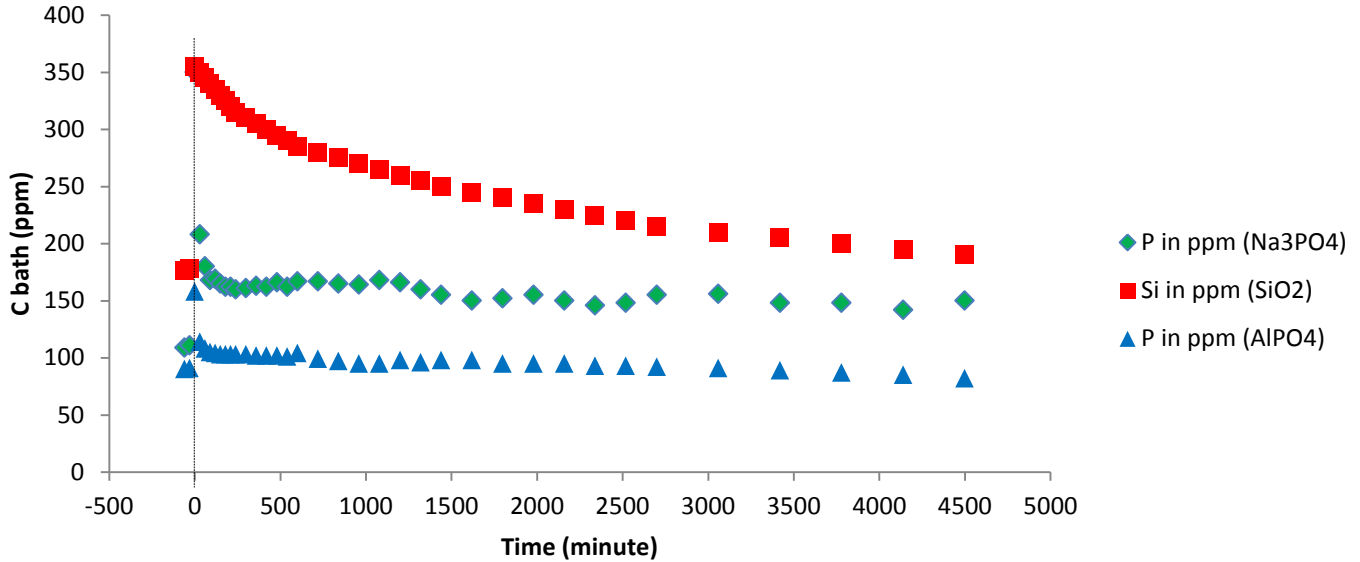


**Figure 5.7:** Distribution of phosphorus and silicon in the bath after the addition. The dotted line marks the time of addition

### P and Si in metal after addition of $\text{AlPO}_4$ , $\text{Na}_3\text{PO}_4$ and $\text{SiO}_2$

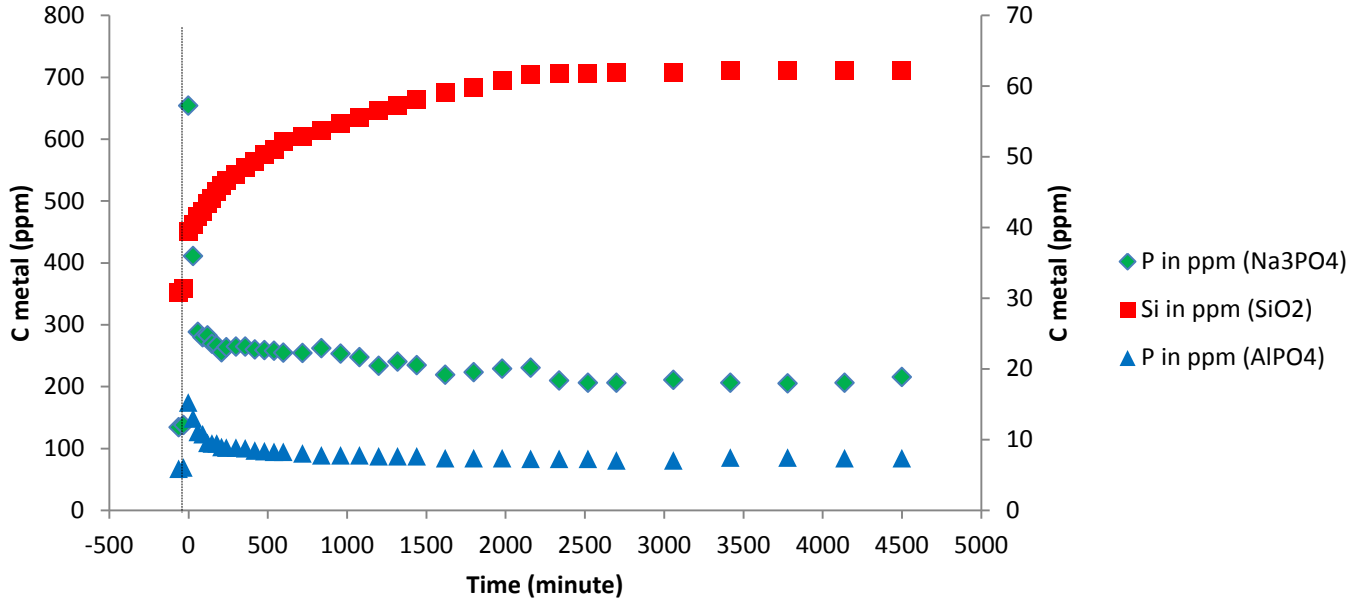
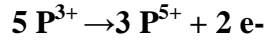
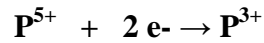


**Figure 5.8:** Distribution of phosphorus and silicon in the bath after the addition. The dotted line marks the time of addition

Part of phosphorus ends up in the metal when going through the red-ox reaction cycle. A great part of the current can be lost due to the fact that phosphorus can be ascribed to this red-ox reaction cycle.



Furthermore, Figure 5.9 illustrates that the decrease in the silicon concentration in the bath over time is a mass transport controlled deposition of silicon at the aluminium cathode. Nearly all of the added silicon is mainly reduced at the cathode.

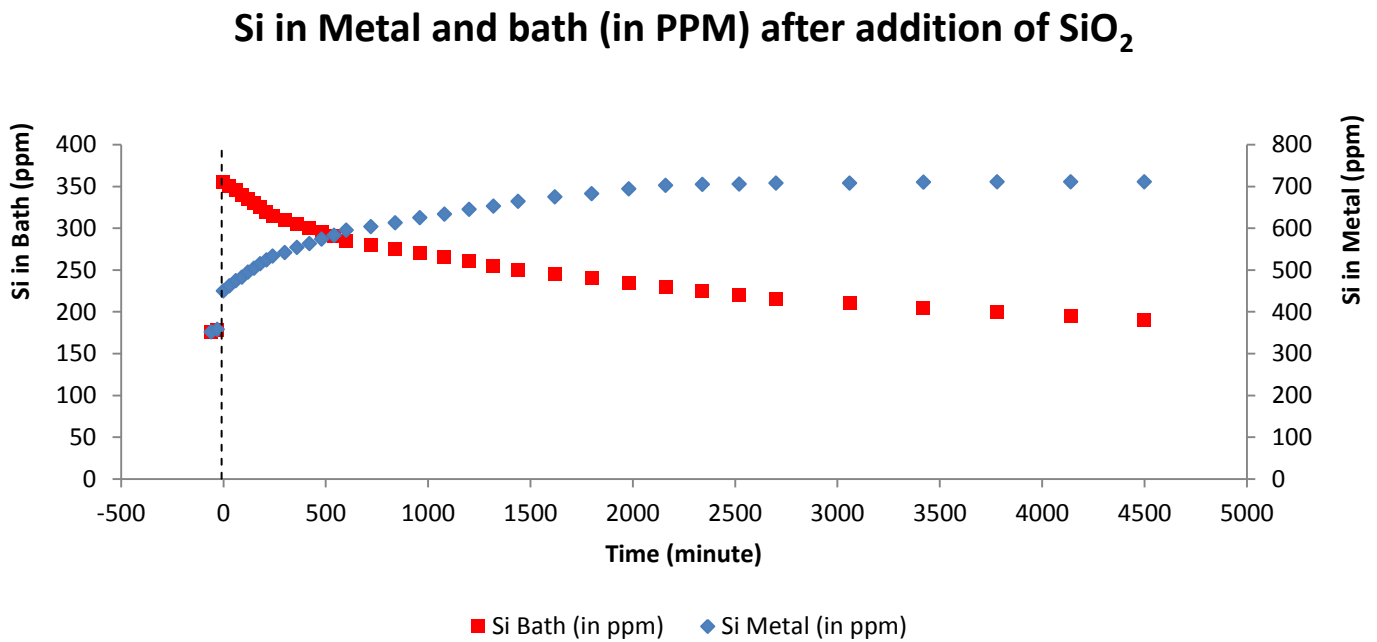


**Figure 5.9:** Distribution of silicon in the metal and bath after the addition. The addition was made at  $t = 0$  minute

### **Equilibrium Distribution Coefficient (K):**

The phosphorus content in the produced metal from industrial cells was exploited to find a relationship with a number of process variables. Analysis of bath and metal for several industrial cells demonstrated that the ratio of the average content of phosphorus in the bath and in the metal was almost constant. The ratio was found to be around 10.

$$K = \frac{\text{Average impurity content in bath (ppm)}}{\text{Average impurity content in aluminium metal (ppm)}}$$

From Figure 5.1 and Figure 5.2:

$$K = \frac{158 \text{ ppm}}{15.2 \text{ ppm}} = 10.4$$

This trend confirms what is known in the literature which is 10 and it is the standard in all aluminium smelters.

## 5.2 Phosphorus and process variables

### Temperature:

It can be affirmed that the temperature influences the concentration of phosphorus in the metal and the bath. This can be seen from Figure 5.10 that the phosphorus concentration in the metal for the prebake cells was roughly between 2-9 ppm. Also, it can be seen that the average bath temperature is 952-962°C. The phosphorus content in the metal shows a striking trend with temperature. A temperature increase leads to a decrease in the concentration of phosphorus in the metal. Figure 5.10 shows a clear correlation between high bath temperature and low phosphorus concentration in the metal and vice versa.

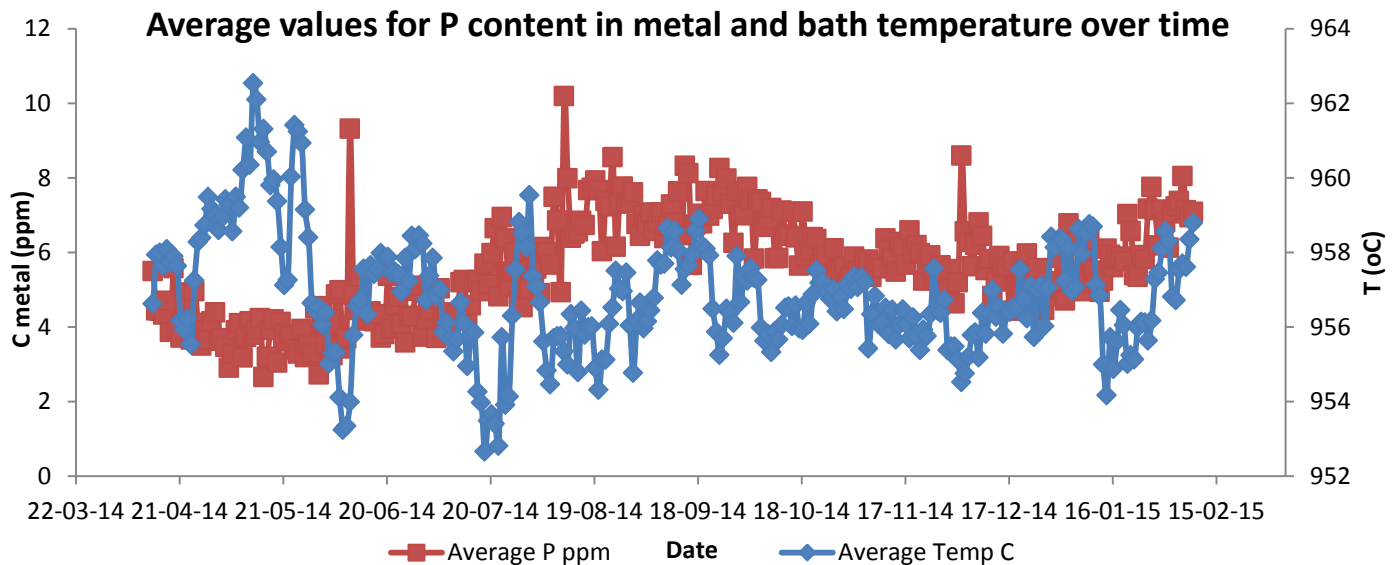


**Figure 5.10:** Average values for the phosphorus content in aluminium and bath temperature over time for prebaked pot-line at QATALUM over a period of 1 year

The high bath temperature causes more phosphorus transfer from the bath to the gas phase. Thus, the phosphorus concentration in the metal is low. Phosphorus evaporation increases with increasing operating temperature. Variations in bath temperature are typically linked with variations in the bath composition.

Also, it is linked with changes of the inter-polar distance (ACD) as well as disturbances such as anode failures or anode effect (AE). These contribute to the low phosphorus concentration in the produced metal.

**Anode Effect (AE):**

Analysis of aluminium metal produced before and after anode effects show that the phosphorus concentration in the metal decreased considerably after the anode effects as seen in Figure 5.11. During this period, the bath temperature is predictably increased. Other consequence than the temperature rise is increased bath convection during anode effect period which possibly will contribute to the low phosphorus concentration in the metal.

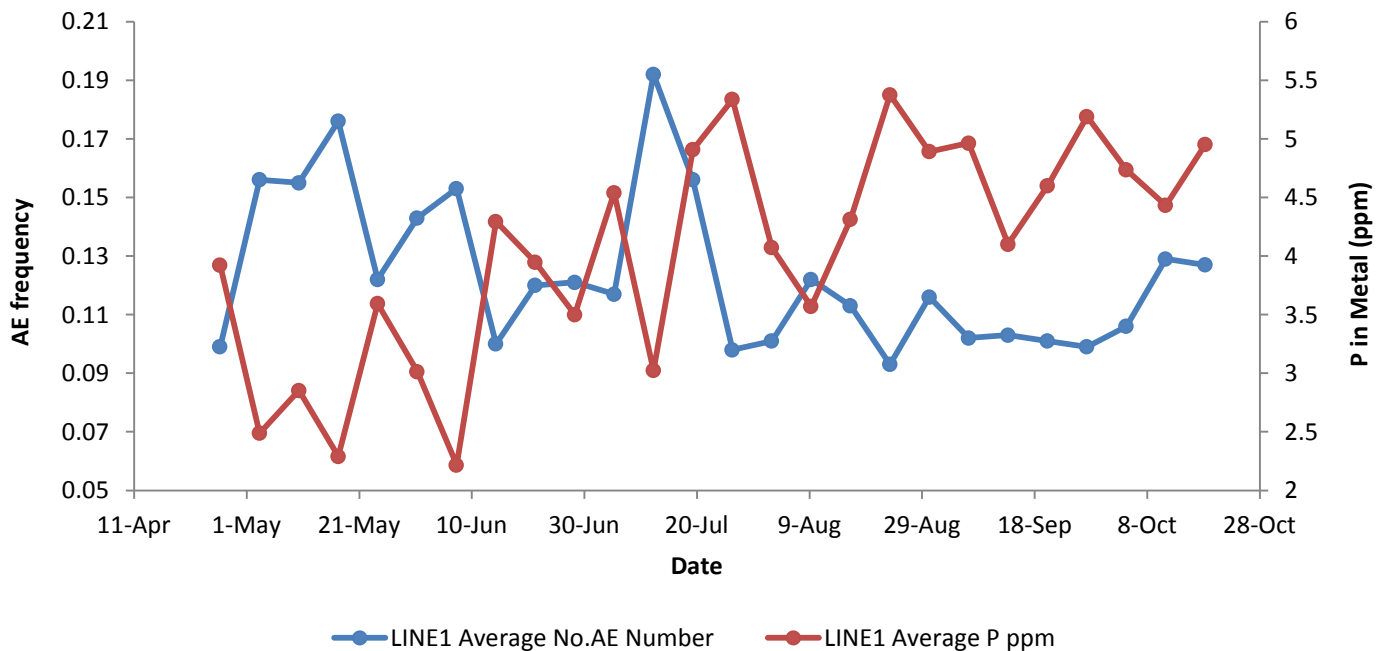


**Figure 5.11:** Correlation between phosphorus concentration in the metal and bath temperature during anode effect

## Start-up:

New electrolyte cells are normally having high bath temperature during the early life of operation. Generally, it was found that the phosphorus concentration was very low during this period. This is due to its high operating temperature (Thermal Behavior) and the variations in electrolyte composition of new cells. It can be noticed from Figure 5.12 that when the bath temperature is eventually reduced, the phosphorus content was found to increase.

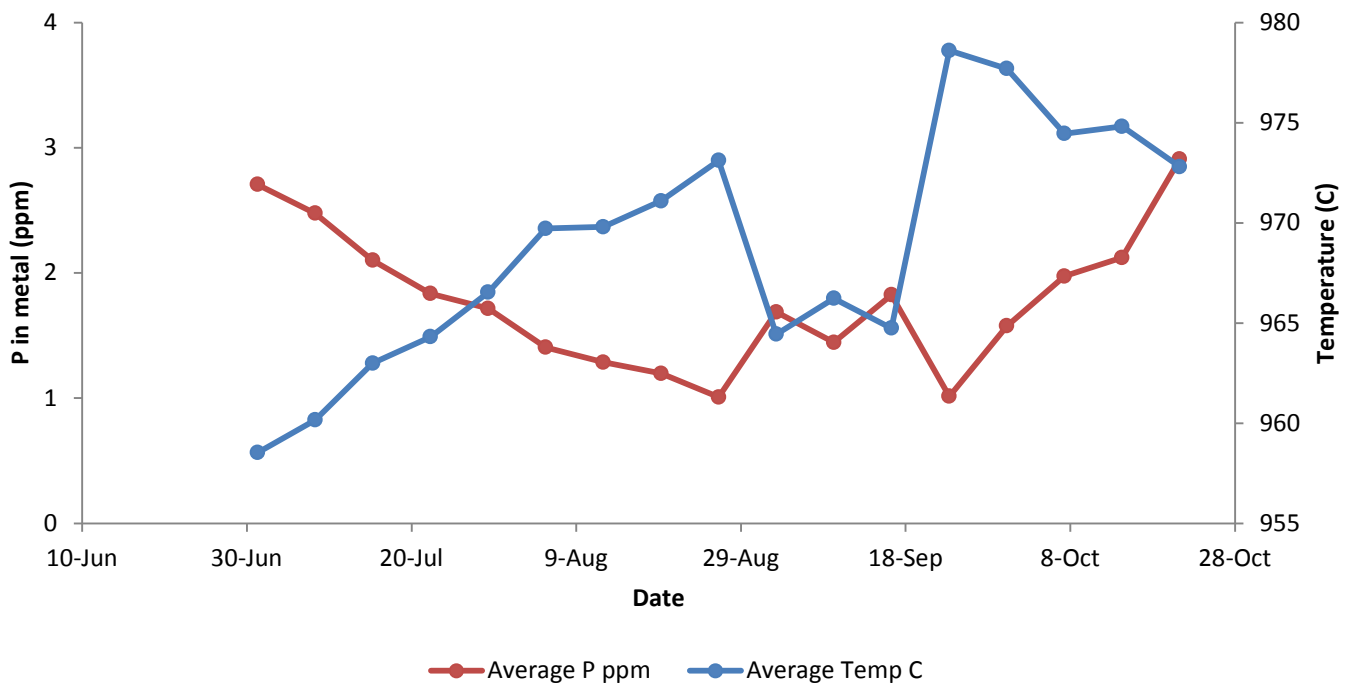


**Figure 5.12:** Correlation between phosphorus concentration in the metal and bath temperature of new cells



### 5.3 Silicon and process variables

#### Temperature:

It is noticeable that the bath temperature influences the silicon concentration in the metal. Figure 5.13 shows a striking trend with temperature. A temperature increase leads to an increase in the concentration of silicon in the metal. Figure 5.13 shows a clear correlation between high bath temperature and high silicon concentration in the metal and vice versa. The high bath temperature causes more silicon transfer from the side ledge of the cell to the bath and metal. Therefore, silicon concentration in the produced metal is high. Less side ledge is found with increasing temperature.

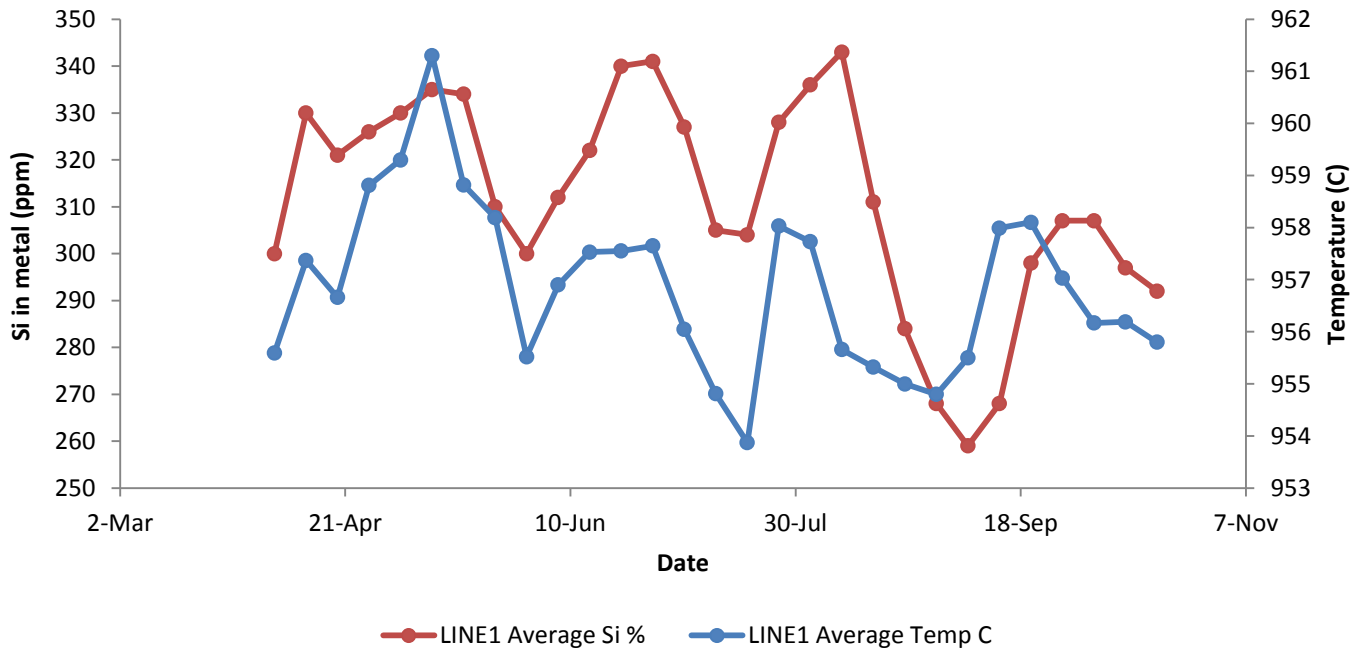


**Figure 5.13:** Average values of the silicon concentration in aluminium and bath temperature over time for prebaked pot-line at QATALUM over a period of 8 months

## Start-up:

New cells normally work at high temperature during the early life of operation. Figure 5.14 shows that the silicon content was very high during this period. This is due to its high operating temperature during this period. When the bath temperature was reduced, the phosphorus content was found to have decreased.

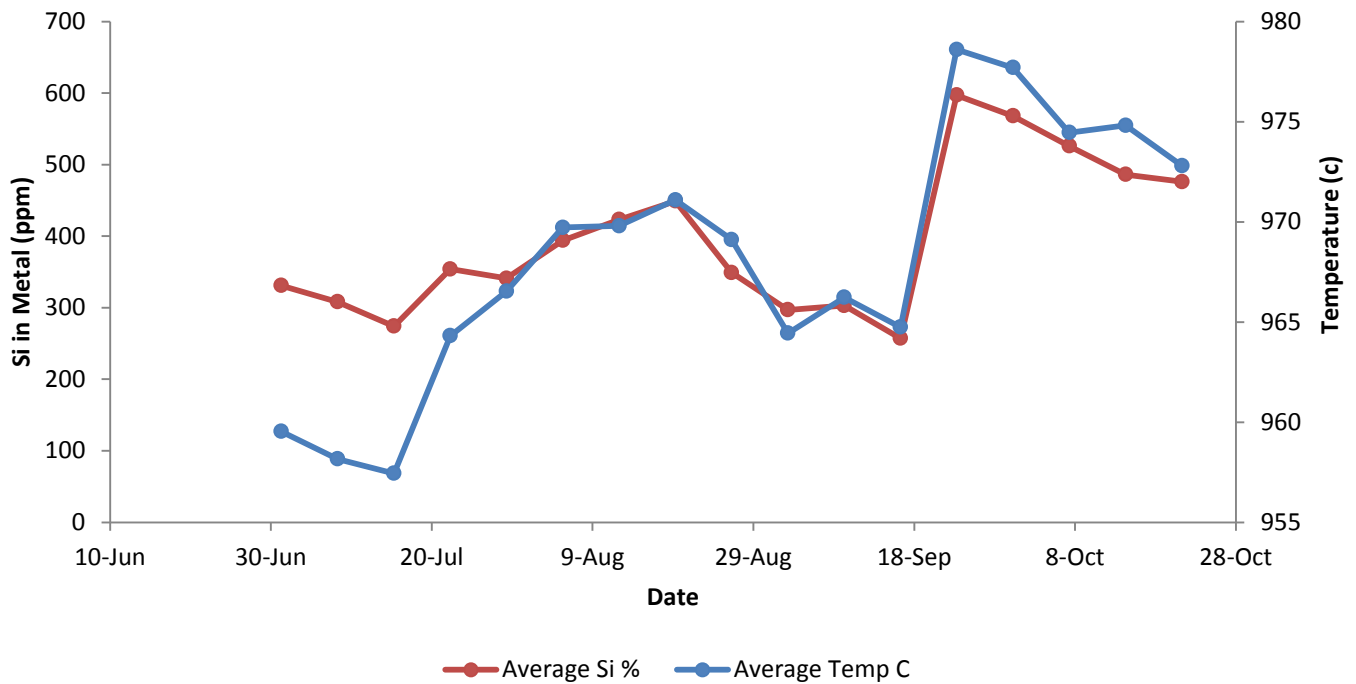


**Figure 5.14:** Correlation between silicon concentration in the metal and bath temperature of new cells

## 5.4 Phosphorus and current efficiency

The possible usage of the sodium concentration on the produced aluminum is a sign for pointing out the current efficiency. It is a remarkable tool for engineers and specialists to assist controlling and analyzing the performance of cells. This indicator is frequently utilized in several aluminum smelters to determine and estimate an exact value on a regular basis. It is difficult to properly find out the mass of aluminum produced on a daily basis for an individual cell. The sodium content in the produced aluminium is well linked to the movement at the electrolyte-metal interface. This movement is extremely effect the current efficiency (%CE). Figure 5.15 shows a solid relationship between the sodium concentration in the produced aluminum and the current efficiency. This correlation in Figure 5.15 was obtained from QATALUM industrial cells.

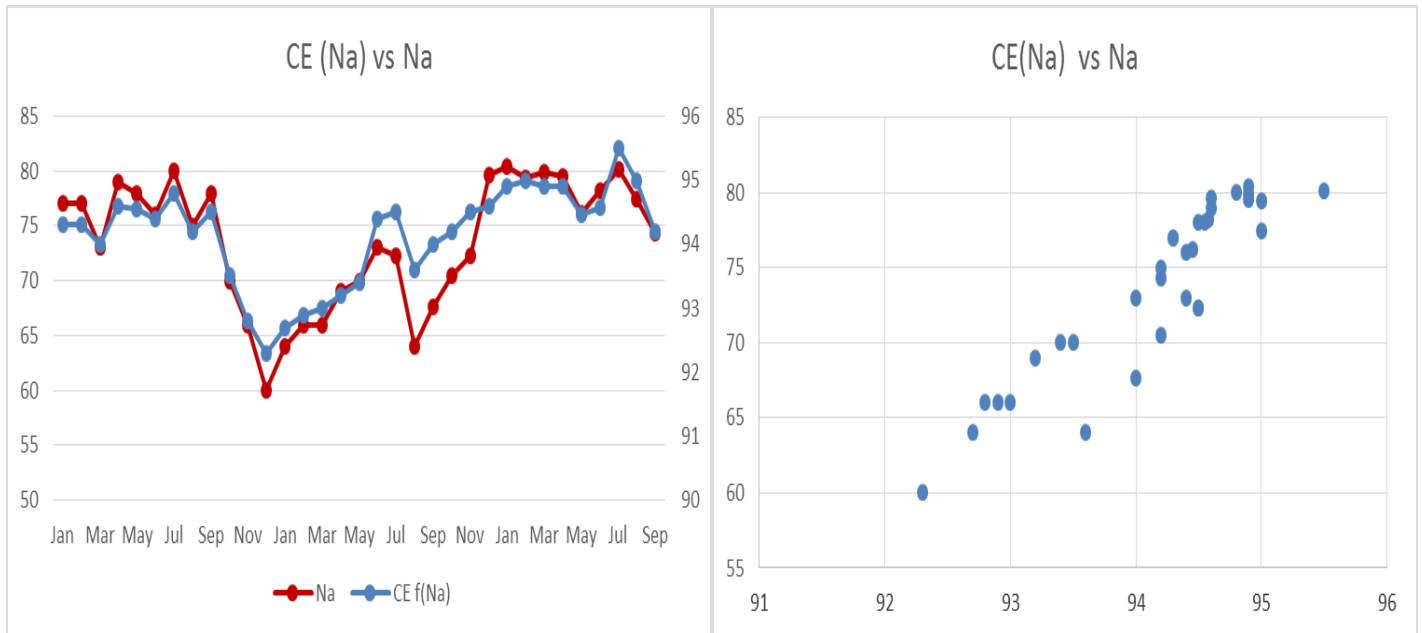


**Figure 5.15:** Correlation between sodium concentration in the produced aluminium and the current efficiency (%CE)

From the above relation, Figure 5.16 was consequently plotted. Figure 5.16 shows the correlation between phosphorus and sodium concentration in the produced metal. There was an inverse relationship between the phosphorus and the sodium concentration in the metal. A phosphorus concentration increases leads to a decrease in the concentration of sodium in the metal and vice versa. Therefore, the high phosphorus

concentration in the metal causes a decrease in the current efficiency of the cell. This trend confirms what is known in the literature and it is the standard in all aluminium smelters.

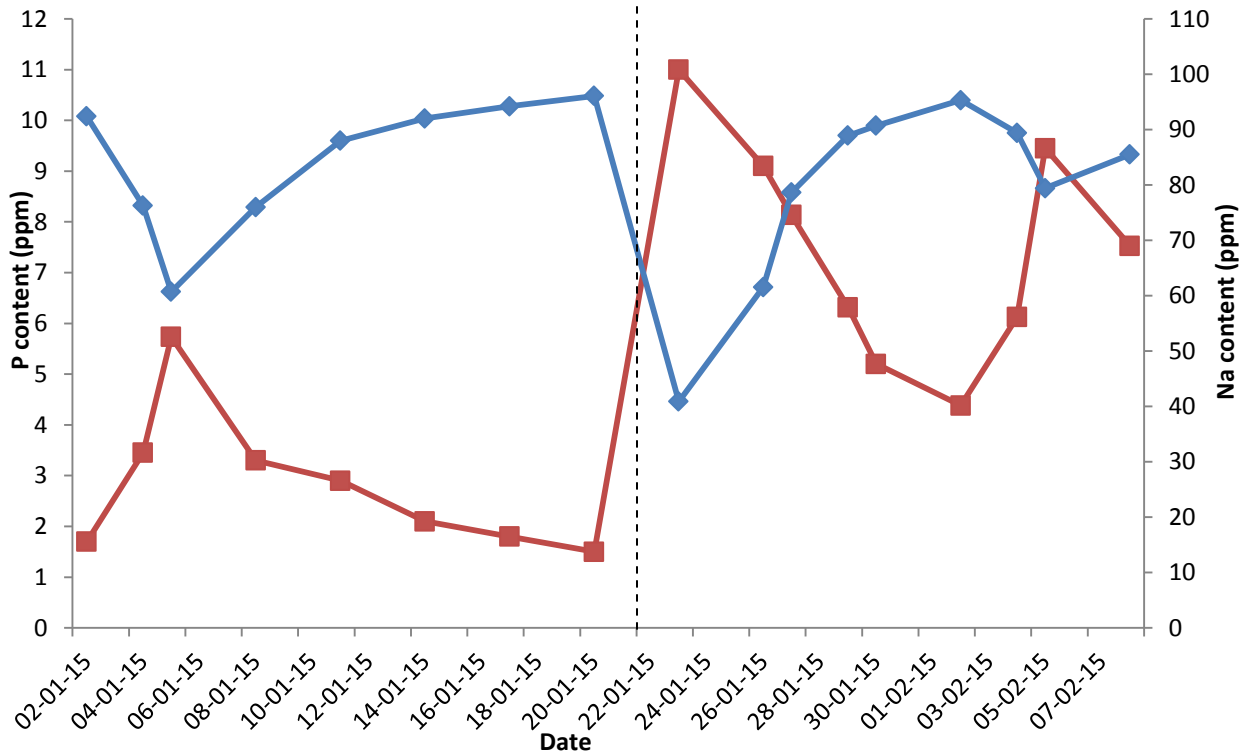


**Figure 5.16:** Correlation between phosphorus and sodium content in the produced metal for the experimental cells. The red line represents the phosphorus concentration. The blue line represents the sodium concentration. The dotted line marks the time of phosphorus compounds addition

## 5.5 Metal Inventory by copper dilution

Changes in metal reservoir between two additions of copper can be used together with tapped metal to find the current efficiency of the electrolyte cells. By adding a certain amount of copper and analyzing copper content in aluminium before and after copper is added, it is possible to calculate the metal reservoir. The metal reservoir is calculated using the following equation:

$$\text{Metal reservoir} = [C_{\text{Cu}} \times M_{\text{Cu}}] / [1000 \times (C_2 - C_1)]$$

Figure 5.17 shows the average values of the metal inventory by copper dilution for the experimental cells at QATALUM over a period of one year. The arrow line marks the time of phosphorus compounds addition. It can be seen from Figure 5.17 that the amount of aluminium metal in the cells reduce by 600 kg after the phosphorus compounds were added in the cells over a period of two weeks. This indicates that phosphorus has an enormous effect on the production of aluminium due to the huge consumption of current ascribed in the red-ox reaction which otherwise be used for aluminium production.

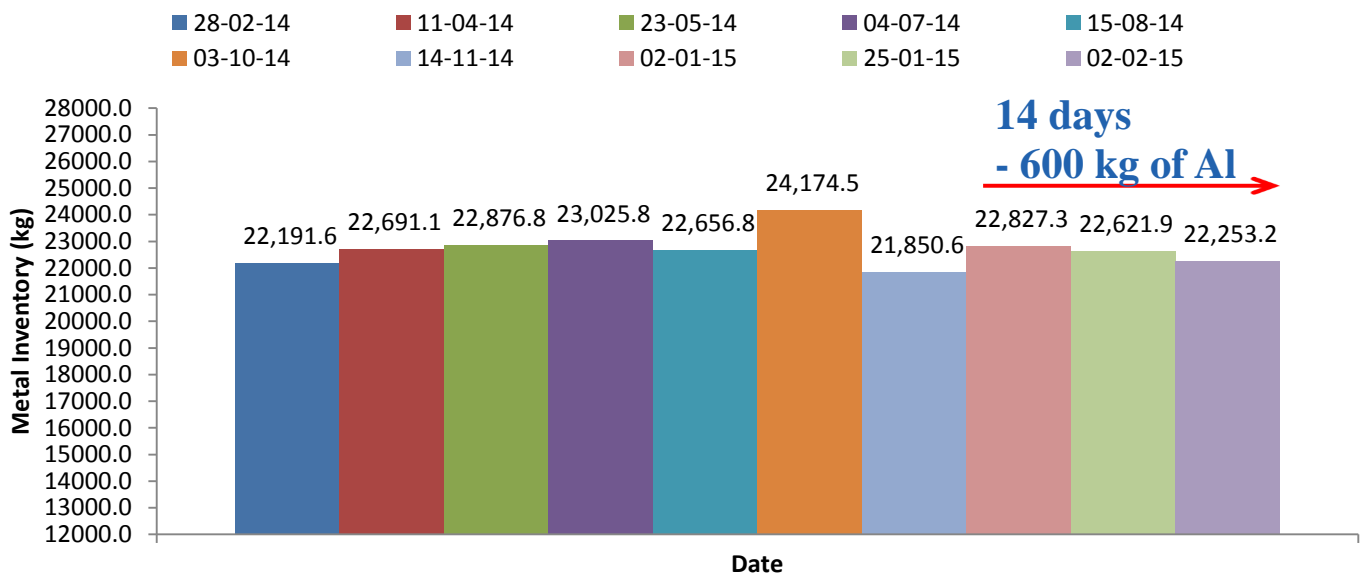


**Figure 5.17:** The average values of the metal inventory by copper dilution for the experimental cells at QATALUM over a period of one year

## 5.6 Current efficiency (%CE) loss calculation

There are two approaches to estimate the current efficiency loss. One method to calculate the %CE loss is metal inventory approach. At QATALUM, the average metal produced per day is 2400 kg per cell. 600 kg were lost during the two weeks of experiment as shown in Figure 5.17. 600 kg per 14 days loss is equal to 42.8 kg loss per day. Therefore, for 94.1 %CE, tap per day 2400 kg:

$$\%CE \text{ loss} = [94.1 \times 42.8] / 2400 = 1.7 \%CE \text{ loss}$$

The second method to calculate the %CE loss is the sodium content in the produced metal approach. The average value of Na in the metal before carried out the experiment is 81 ppm while the average value of Na after the experiment is 67 ppm. Thus, 14 ppm of Na is lost. It can be noticed from Figure 5.15 and Figure 5.18 that the total current efficiency loss during the experiment is 1.7%. The two approaches demonstrate the same results.

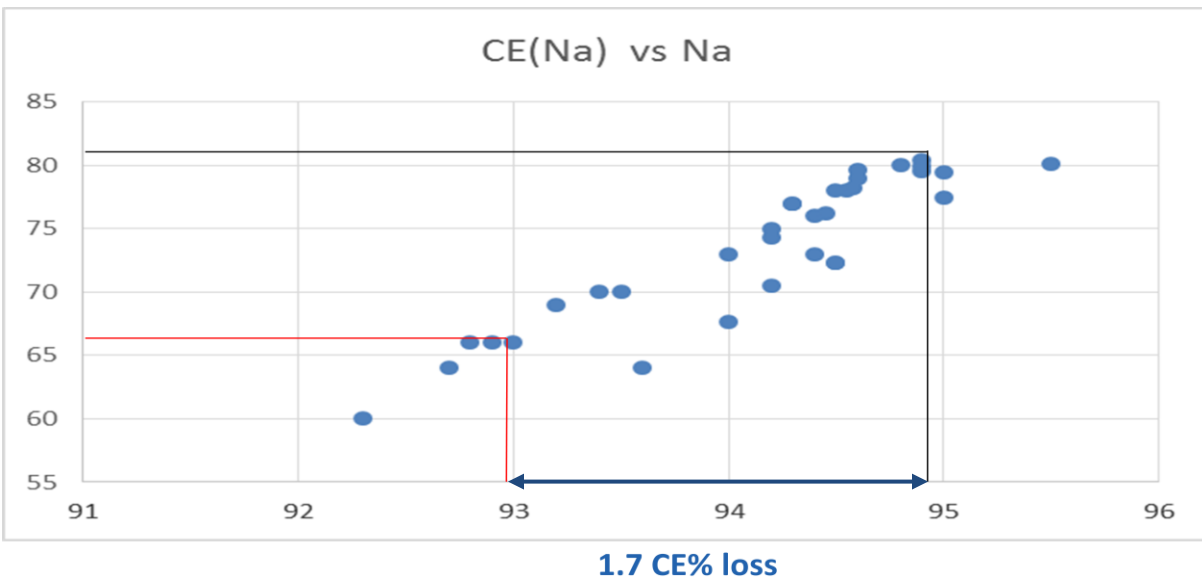


**Figure 5.18:** Correlation between Na concentration in the produced aluminium and the current efficiency (%CE). The black line marks the Na content before the experiment. The red line marks the Na content after the experiment. The blue arrow line marks the total current efficiency loss.

### **%CE Loss Impact on the Financial Results:**

- ❖ QATALUM annual production is 600,000 tonnes.
- ❖ 1% Current Efficiency loss is 6,000 tonnes.
- ❖ 1800 USD per tonne of aluminium is about 10.8 million USD for 6,000 tonnes.

The study shows the cells have lost approximately 2 %CE during the experiment which is equivalent to 18 million USD.

## 5.7 Silicon mass transfer coefficient

Analyses of bath and metal samples as a function of time after additions of certain amounts of impurities were carried out. The concentration of the impurity species can be expressed as follows:

$$C = C_0 \exp \left[ \frac{-A}{V} kt \right]$$

A: Area of the cathode

V: Volume of electrolyte (bath)

C<sub>0</sub>: background concentration

k: Mass Transfer Coefficients

In literature, the mass transfer coefficient is on the range of  $10^{-5}$  -  $10^{-6}$  m/s and it depends on the cell design, technology and operation. Log concentration of silicon in the bath as a function of time after additions of SiO<sub>2</sub> was plotted as shown in Figure 5.19. Solid line is a linear fit of the data.

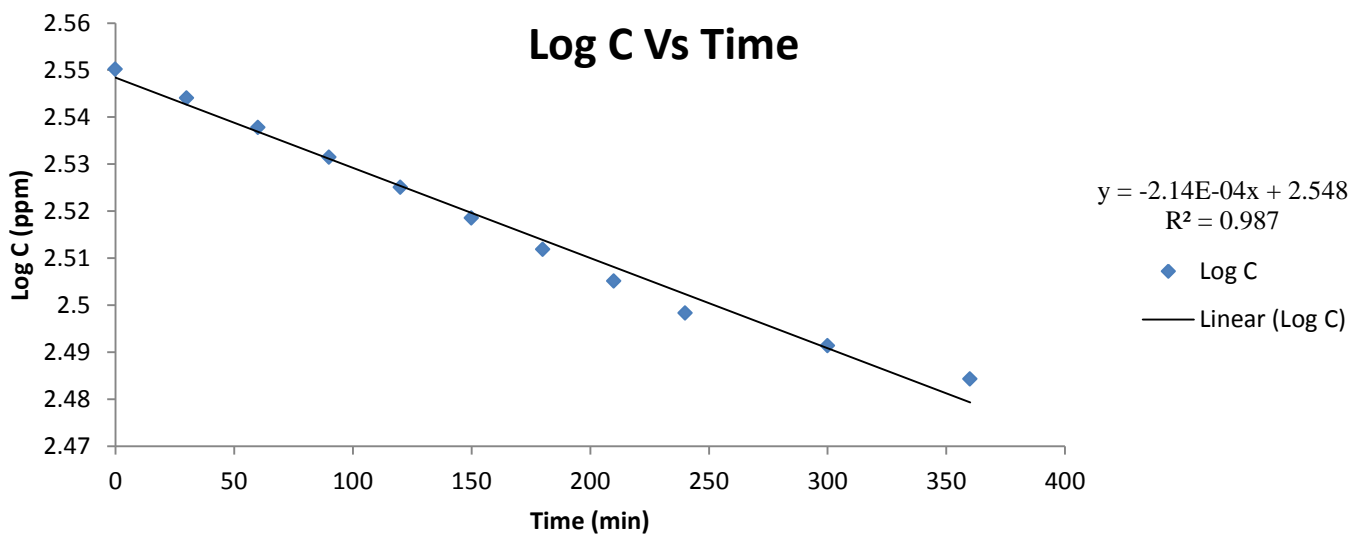


**Figure 5.19:** Log concentration of silicon impurity in the bath as a function of time after additions of SiO<sub>2</sub>



$$C = C_0 \exp \left[ \frac{-A}{V} kt \right]$$

$$\text{Log } C = \text{Log } C_0 - \frac{A}{V} kt$$

$$\frac{\Delta \text{Log } C}{\Delta t} = -\frac{A}{V} k$$



$$\text{Slope of the graph} = -2.14 \times 10^{-4}$$

A: Area of the cathode = 39.75 m<sup>2</sup>

V: Volume of electrolyte (bath) = 5.8 tonnes

Thus, mass transfer coefficient, k can be calculated which is approximately 3.1 x 10<sup>-5</sup> m/s. This trend confirms what is known in the literature which is found to be of the order of 10<sup>-5</sup> - 10<sup>-6</sup> m/s.

## 5.8 Phosphorus Mass balance

For a typical prebake cell at QATALUM, a mass balance concerning phosphorus was derived. The results are summarized in Table 5.1 and Table 5.2 and briefly sketched on Figure 5.20. Also, the full derivations of the phosphorus mass balance are demonstrated in Appendix B. The electrolyte cells are fed with secondary alumina from the dry scrubber. The anodes are covered with a mixture of crushed bath and alumina. Cover materials and solidified bath leave the cells when anodes are changed.

**Table 5.1:** Input

Material	Phosphorus g/tonne Al
Secondary Alumina	19.6
Aluminium Fluoride	1.2
Carbon Anode	3.2
Anode Cover Material	25.7
Soda	0
Calcium Fluoride	0
Total input	49.7

**Table 5.2:** Output

Material	Phosphorus g/tonne Al
Aluminium Metal	6
Carbon Dust	0.6
Excess Tapped Bath	2.8
Mixed Bath Material from Anode Change	20.5
Gas	19.8
Total input	49.7

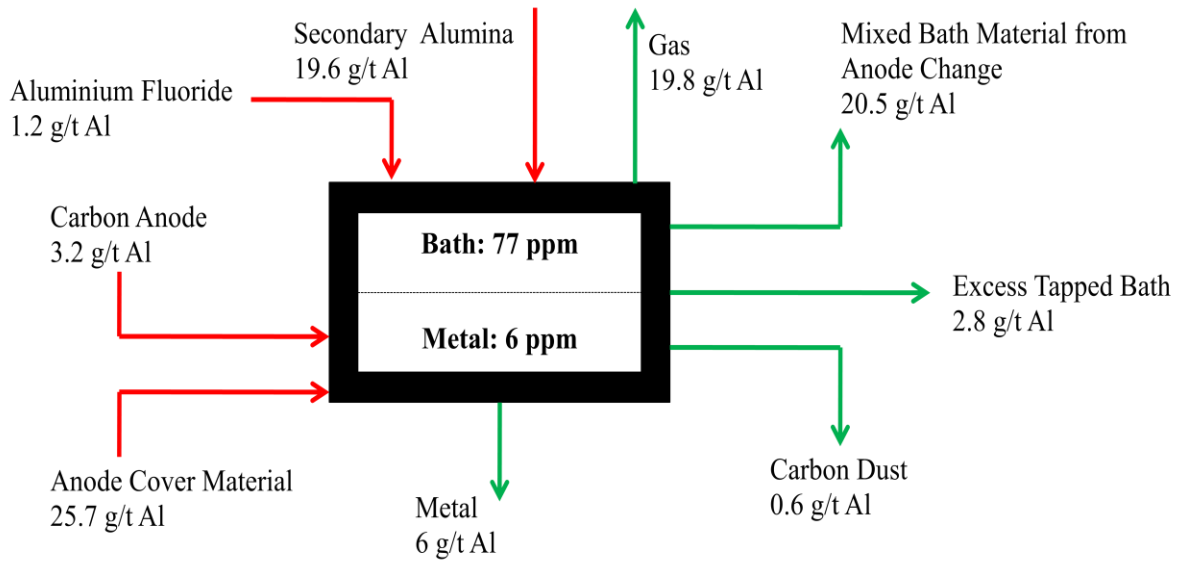


**Figure 5.20:** Mass balance for phosphorus. The phosphorus content in the various mass flows for a typical prebake QATALUM cell

The difference in phosphorus concentration between primary and secondary alumina depends on the amount of phosphorus escaping from the cells with the process gas. High temperature leads to high concentration of carbon dust in the bath which results in an increased amount of phosphorus escaping the cell with process gas or with the covering material. Most of phosphorus in the process gas will be collected in the dry scrubber and recycled to the cells with the secondary alumina. In addition, the phosphorus in the cover material and in the bath removed during anode changing is recycled to the cells as new cover material.

## Chapter 6

### 6. Conclusion

Different impurities were added to the industrial cells to study their behavior. These impurity elements can lower the quality of aluminium and cause reduction on current efficiency. The measurements showed that the retention time of phosphorus in the bath is much longer than for metallic impurities such as silicon. During the start-up and anode effects, the phosphorus and silicon concentrations did not follow a similar concentration pattern. The phosphorus concentration was decreased while the silicon concentration was increased. Data as well showed that the phosphorus concentration in the bath and in the produced aluminium decreases with increasing cell temperature.

Phosphorus behaves differently from other impurities that are nobler than aluminium and a good example is silicon. For metallic impurities nobler than aluminium a mass transport controlled process from bath to metal has been noticed. Mass transfer coefficient for dissolved impurity species is determined for metallic impurities (Si) was found to be of the order of  $10^{-5}$  -  $10^{-6}$  m/s.

The mass balance concerning phosphorus for prebake electrolyte cells was put up. It was found that a large portion of the phosphorus entering the cells is transported with the off-gases to the dry scrubbers. However, since the secondary alumina is used as feeding for the prebake cells, the phosphorus returns and will end up in the produced metal.

According to the results obtained from the measurements, the following a qualitative model for the behavior of phosphorus impurities in the Hall-Héroult cells can be suggested:

- ❖ Phosphorus goes through the process mainly with alumina and is present in the bath as a  $P^{5+}$  or a  $P^{3+}$  species.
- ❖ Phosphorus species may be reduced at the cathode to elemental phosphorus. A possible formation of gaseous phosphorus may be slow because it involves nucleation and growth of gas bubbles. It is more likely that phosphorus will dissolve in the electrolyte. Alloying with aluminium may be little since elemental phosphorus may have a strong tendency to escape into the electrolyte.
- ❖ Phosphorus, reduced to its three valent state by dissolved aluminium, will be oxidized by dissolved  $CO_2$  in the electrolyte or at the anode. Repetitive reduction and oxidation of phosphorus compounds cause a loss in current efficiency with respect to aluminium.
- ❖ Dissolved phosphorus species may also be reduced by impurities in the electrolyte. Small carbon particles (carbon dust) may act as nucleation sites for the formation of adsorbed or solid compounds.
- ❖ Phosphorus species escape with the exit gas and are recycled back to the cells with the secondary alumina. Loss of phosphorus from the cells is mainly due to possible evaporation of phosphorus compounds or due to phosphorus attached to carbon dust that is entrained with the off gases. Evaporation of elemental phosphorus seems to be unlikely due to their reactivity in the presence of air and moisture. Some phosphorus may be lost to the environment with small carbon particles.
- ❖ Increased electrolyte temperature leads to increased escape of phosphorus and decreased phosphorus concentration in produced aluminium.

## Bibliography

1. <http://www.world-aluminium.org/iai/stats/index.asp>.
2. Industrial data from Qatar Aluminium Company (QATALUM), 2011.
3. Thonstad J., Fellner P., Haarberg G. M., Hiveš J., Kvande H., and Sterten Å., Aluminium Electrolysis. Fundamentals of the Hall-Héroult Process 3<sup>rd</sup> ed. 2001, Aluminium-Verlag.
4. Grjotheim K., Krohn C., Malinovský M., Matiašovský K., and Thonstad J., Aluminium Electrolysis. Fundamentals of the Hall-Héroult Process 2<sup>nd</sup> ed. 1982, Aluminium-Verlag.
5. Jentoftsen T. E., *Behaviour of iron and titanium species in cryolite – alumina melts*, Dr. ing. Thesis, NTNU Trondheim, 2000.
6. Augood D. R., *Impurities distribution in alumina reduction plants*, in Light Metals, Proceedings of Sessions 109<sup>th</sup> AIME Annual Meeting, 1980, Las Vegas, Nevada.
7. Vorobyev G. M., Manina A. A., and Moiseev A. P., Tsvet. Met., 1967, **40**(3), p. 60-70.
8. J. Thonstad, P. Fellner, G. M. Haarbeg, J. Hiveš, H. Kvande, Å. Sterten, Aluminium Electrolysis. Fundamentals of the Hall-Héroult Process 3<sup>rd</sup> ed. 2001, Aluminium-Verlag.
9. Fellner P., Ambrová M., Hiveš J., Korenko M., Thonstad J., *Chemical and Electrochemical Reaction of Sulphur Species in Cryolite Melts*, Light Metals, 2005, 570-588.
10. Thonstad J., Nordmo F., Rolseth S., and Paulsen J. B., Light Metals, 1978, 2, p. 460-480.
11. Thisted E. W., *Electrochemical properties of phosphorus compounds in fluoride melts*, Dr. ing. Thesis, NTNU Trondheim, 2003.
12. Zumdahl S. S., *Chemical Principles*, 3<sup>rd</sup> Edition, Houghton Mifflin Company, 1998.
13. Ullman's Encyclopedia of Industrial Chemistry, 6<sup>th</sup> Edition, Willey-VCH, 2003.
14. Daněk V., Chrenková M., Silný A., Staš M., Koniar M., *Long-termed material balance of phosphorus in aluminium reduction cells*, 11<sup>th</sup> International Aluminium Symposium, p. 170-180, September 19-22, 2001, Norway.

15. Brown T. L., Eugene LeMay H., Bursten B. E., *Chemistry – The Central Science*, 8<sup>th</sup> Edition, Prentice – Hall, 2000.
16. Hollemann A. F., Wiberg E., *Lehrbuch der anorganischen Chemie*, Walter de Gruyter, Chapter XIV, 725 ff., 1995.
17. Daněk V., Chrenková M., Silný A., Haarberg G. M., Staš M., *Distribution of phosphorus in industrial aluminium cells*, Proc. Int. TerjeØstvoldSymp., Røros, Norway, p. 160-170, 1998.
18. Daněk V., Chrenková M., Silný A., Haarberg G. M., Staš M., *Distribution of phosphorus in industrial cells*, Can. Met. Quart., 38 (3), 145-157, 1999.
19. Tkatcheva O., Mediaas H., Østvold T., *Phosphorus in cryolite I*, internal report at the Institute of Inorganic Chemistry, NTNU Trondheim, Norway, 1999.
20. Tkatcheva O., Mediaas H., Østvold T., *Phosphorus in cryolite II*, internal report at the Institute of Inorganic Chemistry, NTNU Trondheim, Norway, 1999.
21. Chaudhuri K. B., *Beeinflussung der Aluminiumverluste in Kryolith-Tonerde-Schmelzendurchbadverunreinigungen und Badzusätze*, Ph.D. thesis, Technical University in Berlin, 1968.
22. Grjotheim K., Welch B., *Aluminium Smelter Technology*, 2<sup>nd</sup> Edition, Aluminium-Verlag, Düsseldorf, 1980.
23. Øye H. A., *Impurities in Aluminium Smelting*, 5<sup>th</sup> Australian-Asian Aluminium Smelter Technology Workshop, Sydney, Australia, October 22-27, 660-680, 1995.
24. Richards N., *Alumina in Smelting*, the 19<sup>th</sup> International Course on Process Metallurgy of Aluminium, Chapter 11, Trondheim, Norway.
25. Industrial data from Norsk Hydro Aluminium, 2002.
26. Deininger L., Gerlach J., *Stromausbeutemessungen bei der Aluminium-oxidreduktionselektrolyse in Laboratoriumszellen*, Metall, 33, 2, 1979, 130-140.

27. Qiu Z., Yu Y., He M., Yu X., Li B., *Impurity distribution in bath and metal in aluminium electrolysis*, Aluminium, 75, 12, 1999, 1100-1120.
28. Sturm E., Wedde G., *Removing impurities from the aluminium electrolysis process*, Light Metals 1998, 230-240.
29. Solli P. A., *Current efficiency in aluminium electrolysis cells*, Dr. ing. Thesis, NTNU Trondheim, Norway, 1993.
30. Cuthall E. R., *Removal of phosphorus from dry scrubber alumina*, Light Metals, 1979, 925-935.
31. Lossius L. P., Øye H. A., *Removing impurities from secondary alumina fines*, Light Metals, 1992, 245-260.
32. Haugland E., Haarberg G. M., Thisted E., Thonstad J., *The behavior of phosphorus impurities in aluminium electrolysis cells*, Light Metals, 2001, 549-553.
33. Oblakowski R., Pietrzyk S., *Superheating of  $Na_3AlF_6-AlF_3-Al_2O_3$  electrolyte in the process of aluminium electrolysis*, Metallurgy and Foundry Engineering, **21**(3), 170-185, 1995.
34. Böhm E., Reh L., Sparwald V., Winkhaus G., *Removal of impurities in aluminium smelter dry gas cleaning using the VAW/Lurgi process*, Light Metals, 1976, 505-525.
35. Augood D. R., *Impurities distributions in alumina reduction plants*, Light Metals, 1980, 410-430.
36. Handå S., *The effect of phosphorus on aluminium cells connected to dry scrubbers*. Problems caused by phosphorus in the prebake line at KUBAL Smelter in Sundsvall Sweden, Unpublished report, July 2000.
37. Homsí P., the 18<sup>th</sup> International Course on Process Metallurgy of Aluminium, Trondheim, Norway 1999.
38. Sommers M. A., *Understanding the Elements of the Periodic Table – Silicon*, the Rosen Publishing Group, 2008.



39. Meirbekova R., Thonstad J. and Haarberg G. M., Saevarsdottir G., *Effect of Current Density and Phosphorus Species on Current Efficiency in Aluminum Electrolysis at High Current Densities*, Light Metals 2014
40. Thonstad J., Utigard T., Vogt H., *On the Anode Effect in Aluminum Electrolysis*, Light Metals, 2000,131 -137
41. Meirbekova R., Saevarsdottir G., Armoo J. P. and Haarberg G. M., *Effects of current density and phosphorus impurities on the current efficiency for Aluminum deposition in cryolite-alumina melts in a laboratory cell*, in proceedings, Molten Salts 9, Trondheim June 2011.
42. Meirbekova R., Saevarsdottir G., Armoo J. P. and Haarberg G. M., *Effects of current density and phosphorus impurities on the current efficiency for Aluminum deposition in cryolite-alumina melts in a laboratory cell*, Light Metals 2013, The Metals Materials and Mineral Society.
43. Geay P. Y., Welch B. J., Homsy P., *Sludge in operating aluminium smelting cells*, Light Metals 2001, 541-547.
44. Haupin W., *The principle of aluminium electrolysis*, The 19<sup>th</sup> International Course on Process Metallurgy of Aluminium, Chapter 2, Trondheim, Norway, 2000.
45. Bard A. J., Faulkner L. R., *Electrochemical methods*, John Wiley & Sons, New York, 2<sup>nd</sup> ed., 2001.
46. Rolseth S., Moxnes B., Gangstad A., *Method for determination of volume of liquid bath in Hall-Héroult cells*, 11<sup>th</sup> International Aluminium Symposium, Sept. 19.-22., Trondheim-Bergen-Trondheim, Norway, 2001.
47. Aluminium Handbook 2 – Forming, Casting, Surface Treatment, Recycling and Ecology, Aluminium Verlag 2003.
48. Thisted E. W., Haarberg G. M., Thonstad J., *Solubility of  $AlPO_4$  in cryolite melts*, ThermochemicaActa, 447, 2006, 41-44.

49. Martinez A. M., Haarberg G. M., Kvalheim E., Zhao D., Rolseth S., *Electrochemical behavior of dissolved iron species in molten salts*, Euchem conference on Molten Salts and Ionic Liquids, September 16-22, 2006, Hammamet, Tunisia.
50. Nogita K., Schaffer P. L., McDonald S. D., Lu L., Dahle A. K., *Modification of Al-Si alloys*, Aluminium, 4, 81, 2005, 330.
51. Gupta C. K., *Chemical Metallurgy – Principles and Practice*, Wiley – VCH, 2003.

## Appendix A

**Table 1.1:** Impurity concentrations in different raw material [2]

<b>Impurity</b>	<b>Al<sub>2</sub>O<sub>3</sub> (wt.%)</b>	<b>AlF<sub>3</sub> (wt.%)</b>
<b>SiO<sub>2</sub></b>	0.009	0.15
<b>Fe<sub>2</sub>O<sub>3</sub></b>	0.006	0.01
<b>TiO<sub>2</sub></b>	0.004	
<b>CaO</b>	0.036	
<b>ZnO</b>	<0.001	
<b>V<sub>2</sub>O<sub>5</sub></b>	<0.001	
<b>P<sub>2</sub>O<sub>5</sub></b>	<0.001	0.014
<b>Cr<sub>2</sub>O<sub>3</sub></b>	<0.001	
<b>Ga<sub>2</sub>O<sub>3</sub></b>	0.004	
<b>Na<sub>2</sub>O</b>	0.41	0.12
<b>K<sub>2</sub>O</b>	<0.001	
<b>SO<sub>4</sub></b>		0.26

**Table 1.2:** Impurity concentrations in different raw materials [2]

<b>Impurity</b>	<b>Liquid Pitch (ppm)</b>	<b>Petroleum Coke (ppm)</b>
<b>Si</b>	33	51
<b>Fe</b>	74	54
<b>Pb</b>	102	
<b>Zn</b>	83	
<b>V</b>		171
<b>Na</b>	52	28
<b>Ni</b>		73
<b>Ca</b>	40	36
<b>S</b>	0.5 wt.%	2.93 wt.%
<b>Ash</b>	0.1 wt.%	0.08 wt.%

**Table 2.3:** Laboratory data for the distribution coefficients between bath and metal for several impurities, impurity level A equals 0.0025wt.% P, 0.02 wt.% Si and 0.01 wt.% Fe in the bath, impurity level 2A equals twice the impurity concentrations of A and so for impurity fourth and eighth [27].

Impurity level	Type of experiment (Duration 4 hours)	Distribution coefficients for various impurities		
		P	Si	Fe
A	No electrolysis	0.81	0.662	0.147
	Electrolysis	-	0.602	0.147
2A	No electrolysis	0.833	0.681	0.084
	Electrolysis	0.764	0.277	0.134
4A	No electrolysis	0.871	0.383	0.105
	Electrolysis	0.815	0.233	0.102
8A	No electrolysis	1	0.367	0.221
	Electrolysis	-	0.091	0.069

**Table 2.5: Input [14]**

<b>Material</b>	<b>Year</b>	<b>Phosphorus (ppm)</b>	<b>Phosphorus g/tonne Aluminium</b>
<b>Primary Al<sub>2</sub>O<sub>3</sub></b>	1997	3.8	7.3
	1998	4.4	8.5
	1999	3.7	7.0
<b>AlF<sub>3</sub></b>	1997	92.0	1.6
	1998	93.3	1.4
	1999	77.9	1.0
<b>Anodes</b>	1997	5.1	2.6
	1998	2.3	1.2
	1999	4.4	2.4
<b>Covering Material</b>	1997	34.0	12.4
	1998	67.0	23.2
	1999	45.0	14.6
<b>Total input</b>	1997		23.8
	1998		34.3
	1999		25.0

**Table 2.6:** Recycling material and bath [14]

<b>Material</b>	<b>Year</b>	<b>Phosphorus (ppm)</b>	<b>Phosphorus g/tonne Aluminium</b>
<b>Bath</b>	1997	38.7	
	1998	42.6	
	1999	67.1	
<b>Anode gas</b>	1997		56.1
	1998		42.2
	1999		29.4
<b>Secondary Al<sub>2</sub>O<sub>3</sub></b>	1997	33.0	63.4
	1998	26.0	50.7
	1999	19.0	26.4

**Table 2.7: Output [14]**

<b>Material</b>	<b>Year</b>	<b>Phosphorus (ppm)</b>	<b>Phosphorus g/tonne Aluminium</b>
<b>Aluminium metal</b>	1997	3.5	3.5
	1998	4.3	4.3
	1999	6.5	6.5
<b>Emissions</b>	1997		2.8
	1998		2.1
	1999		1.5
<b>Covering</b>	1997	97.0	15.6
	1998	176.0	26.7
	1999	119.0	16.9
<b>Anode Butts</b>	1997	2.7	0.2
	1998	2.7	0.3
	1999	2.7	0.4
<b>Total output</b>	1997		22.1
	1998		33.4
	1999		25.2



**Table 2.8:** Phosphorus mass balance at Soderberg cells fed by primary Al<sub>2</sub>O<sub>3</sub> [11]

<b>Material</b>	<b>Phosphorus g/tonne Aluminium</b>
<b>Primary Al<sub>2</sub>O<sub>3</sub></b>	9.6
<b>Anodes</b>	3.5
<b>AlF<sub>3</sub></b>	3.1
<b>Metal</b>	2.0
<b>Dust emissions</b>	2.9
<b>Gas emissions</b>	11.3
<b>Bath phosphorus (ppm)</b>	55

## Appendix B

### Mass Balance Estimation:

#### Input:

##### 1- Secondary Alumina:

Secondary alumina was analyzed in the lab and it was found that the phosphorus pent-oxide ( $P_2O_5$ ) content is 0.0023%.

Secondary alumina used per day for 94.1 %CE:

$$94.1 = \frac{\text{actual production}}{8.053 \times 314.5}$$

Actual production = 2383.24 kg/day

Thus, alumina used =  $1.95 \times 2383.24 = 4647$  kg/day

$$\text{Amount of phosphorus (P) in phosphorus pent-oxide (P}_2\text{O}_5) = \frac{31 \times 2}{31 \times 2 + 16 \times 5} = 0.436$$

$$\text{Thus, the amount of phosphorus per day} = \frac{4647 \times 0.0023 \times 0.436}{100} = 0.0466 \text{ kg/day} = 46.6 \text{ g/day}$$

The average aluminium metal produced per day for one cell is 2.383 tonne.

$$\text{Thus, the average total amount of phosphorus} = \frac{46.6}{2.383} = 19.6 \text{ g/tonne of aluminium}$$

##### 2- Aluminium Fluoride:

From the supplier specification, it was found that the phosphorus pent-oxide ( $P_2O_5$ ) content is 0.014%.

For 11 to 13 wt% excess  $AlF_3$  in cell, an average of 45 kg of  $AlF_3$  used per day.

Thus, the amount of phosphorus per day =  $\frac{45 \times 0.014 \times 0.436}{100} = 0.00274 \text{ kg/day} = 2.74 \text{ g/day}$

The average aluminium metal produced per day for one cell is 2.383 tonne.

Thus, the average total amount of phosphorus =  $\frac{2.74}{2.383} = 1.2 \text{ g/tonne of aluminium}$

### **3- Carbon Anode:**

The carbon anode was analyzed in the lab and it was found that the phosphorus content is 0.0008%.

The net consumption of anode per tonne of aluminium = 400 kg/tonne

The average aluminium metal produced per day for one cell is 2.383 tonne.

Anode carbon used per day =  $400 \times 2.383 = 953.2 \text{ kg/day}$

The amount of phosphorus per day =  $\frac{953.2 \times 0.0008}{100} = 0.007625 \text{ kg/day} = 7.625 \text{ g/day}$

Thus, the average total amount of phosphorus =  $\frac{7.625}{2.383} = 3.2 \text{ g/tonne of aluminium}$

### **4- Anode Cover Material:**

The anode cover materials were analyzed in the lab and it was found that the phosphorus content is 0.009%.

An average amount of anode cover materials used per pair of anode = 680 kg/pair of anode

The amount of phosphorus =  $\frac{680 \times 0.009}{100} = 0.0612 \text{ kg} = 61.2 \text{ g}$

The average aluminium metal produced per day for one cell is 2.383 tonne.

Thus, the average total amount of phosphorus =  $\frac{61.2}{2.383} = 25.7 \text{ g/tonne of aluminium}$

## **Output:**

### **1- Aluminium Metal:**

The aluminium metal was analyzed in the lab and it was found that the phosphorus content is 0.0006%.

The average aluminium metal produced per day for one cell is 2.383 tonne.

The amount of phosphorus =  $\frac{2.383 \times 0.0006 \times 1000}{100} = 0.00143 \text{ kg/day} = 14.3 \text{ g/day}$

Thus, the average total amount of phosphorus =  $\frac{14.3}{2.383} = 6 \text{ g/tonne of aluminium}$

### **2- Carbon Dust:**

An average of 3.75 tonnes of carbon per day for all cells

There are 457 anode changes per day for whole 2 pot-lines

The amount of carbon per anode change =  $\frac{3.75 \times 1000}{457} = 8.2 \text{ kg/anode change} = 8200 \text{ g/anode change}$

Carbon dust was analyzed in the lab and it was found that the phosphorus pent-oxide ( $\text{P}_2\text{O}_5$ ) content is 0.04%.

Amount of phosphorus (P) in phosphorus pent-oxide ( $\text{P}_2\text{O}_5$ ) =  $\frac{31 \times 2}{31 \times 2 + 16 \times 5} = 0.436$

The amount of phosphorus per day =  $\frac{8200 \times 0.04 \times 0.436}{100} = 1.43 \text{ g/day}$

Thus, the average total amount of phosphorus =  $\frac{1.43}{2.383} = 0.6 \text{ g/tonne of aluminium}$

### 3- Excess Tapped Bath:

An average of 60 tonnes of bath is tapped per day for all cells.

The bath was analyzed in the lab and it was found that the phosphorus content is 0.0077%.

$$\text{The amount of phosphorus} = \frac{60 \times 0.0077 \times 1000}{100} = 4.62 \text{ kg/day} = 4620 \text{ g/day}$$

$$\text{Thus, the average total amount of phosphorus} = \frac{4620}{2.383} = 1938.7 \text{ g/tonne of aluminium}$$

$$\text{For one cell} = \frac{1938.7}{704} = 2.8 \text{ g/tonne of aluminium}$$

### 4- Mixed Bath Material from Anode Change:

Mixed bath material from anode change was analyzed in the lab and it was found that the phosphorus pent-oxide ( $\text{P}_2\text{O}_5$ ) content is 0.017%.

An average mass of cavity material is 660 kg.

$$\text{The amount of phosphorus} = \frac{660 \times 0.017 \times 0.436}{100} = 0.0489 \text{ kg/cavity material} = 48.9 \text{ g/cavity material}$$

$$\text{Thus, the average total amount of phosphorus} = \frac{48.9}{2.383} = 20.5 \text{ g/tonne of aluminium}$$

### 5- Gas:

In any system, the input should be equivalent to the output. As the input are 49.7 g/tonne of aluminium; thus, the output is 49.7 g/tonne of aluminium.

Output = Aluminium Metal + Carbon Dust + Excess Tapped Bath + Mixed Bath Material from Anode Change + Gas

$$49.7 = 6 + 0.6 + 2.8 + 20.5 + \text{Gas}$$

Thus, the average total amount of phosphorus = 19.8 g/tonne of aluminium